PSD
Supplemental Information

ESRL Physical Sciences Laboratory Review

David Skaggs Research Center
Boulder, Colorado
March 9-12, 2010

PSD Income by Fiscal Year

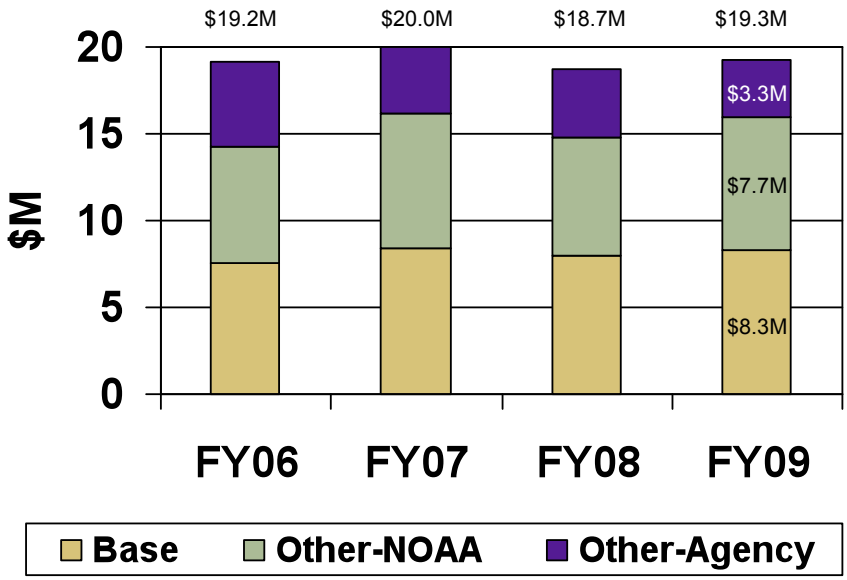

FY09 PSD Income by NOAA Goal

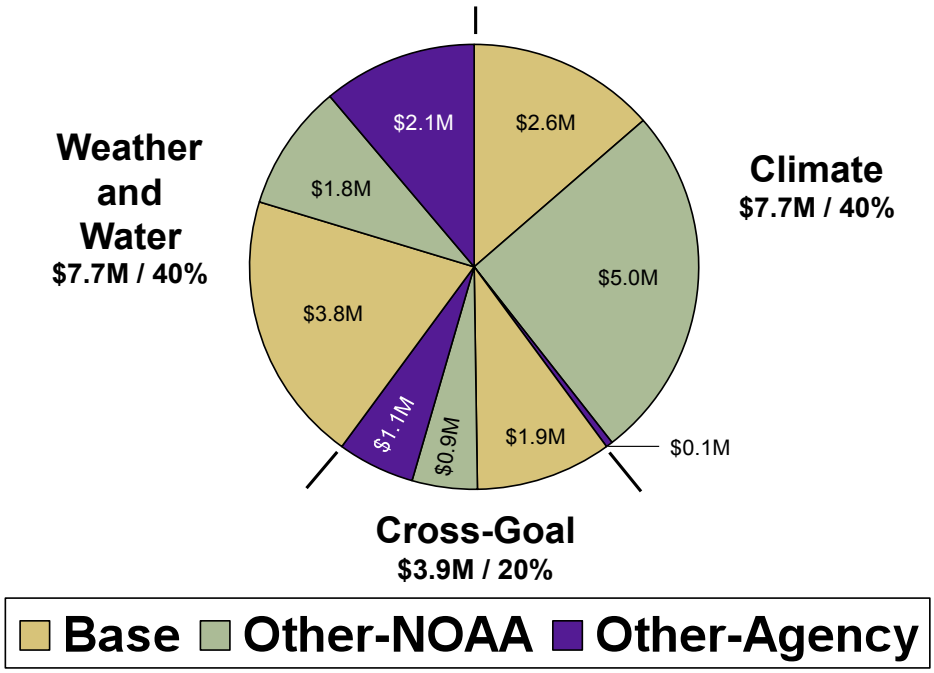

PSD Income by Fiscal Year

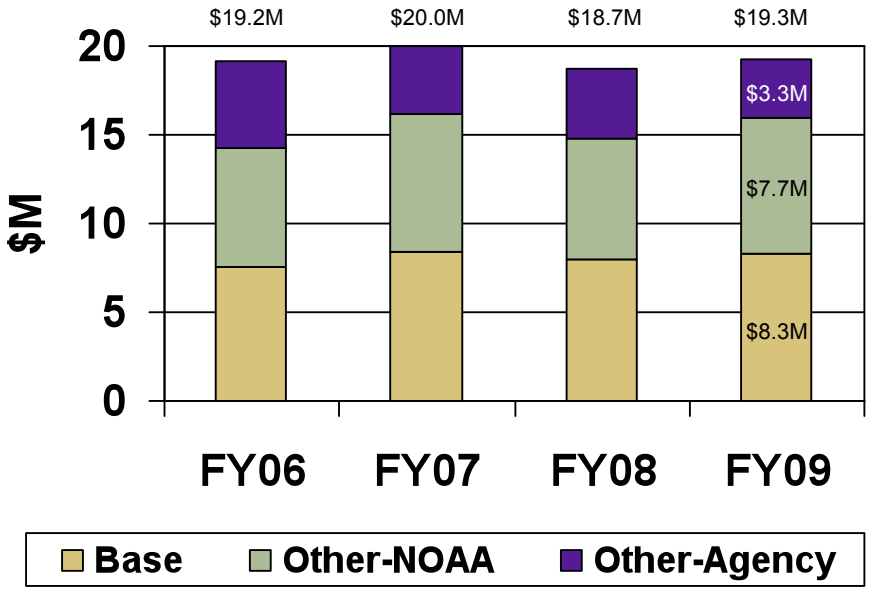

FY09 PSD Expenses by Category

(Total ≈ $19.3M)

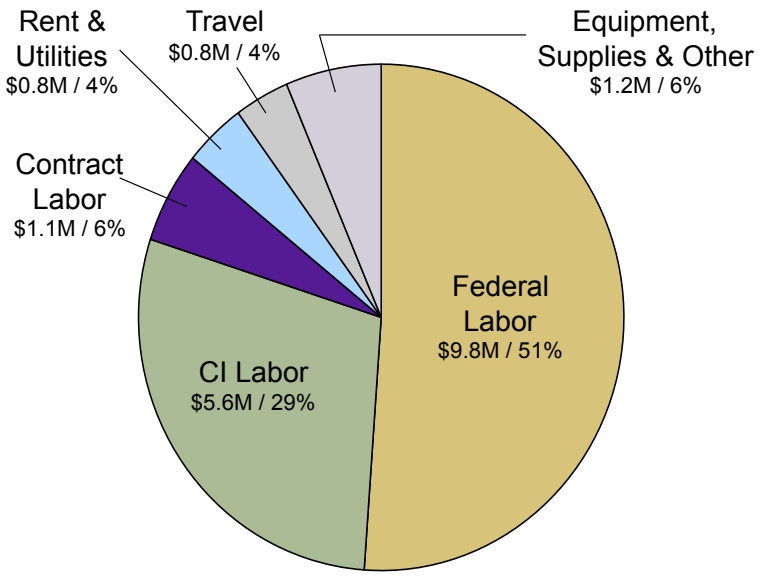

PSD Staffing by Fiscal Year

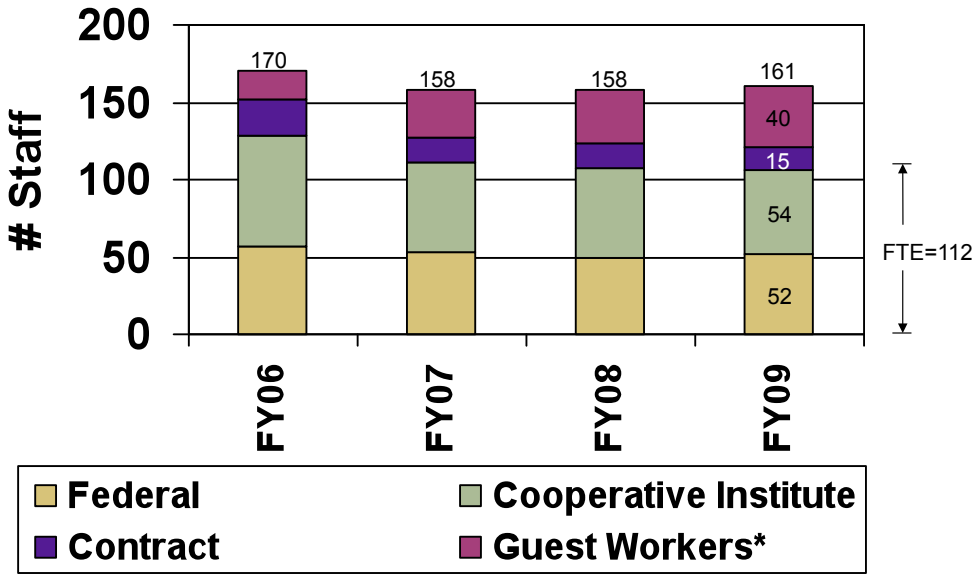

*Guest Workers include: Scientists Emeriti (3), Guest Scientists (25), Post-docs (6), Guest Students (4), Externally Supported Staff (2)

FY09 PSD Organization

Director's Office

Directorate
Budget and Administration Group
Information Technology Group
Communication Group

Research Partnership Programs

National Integrated Drought Information System (NIDIS)
Western Water Assessment (WWA)
Advanced Sensor Applications Program (ASAP)
University of Colorado –
Center for Environmental Technology (CET)
Special Projects (SP)

Climate Analysis Branch

Climate Dynamics Team
Attribution and Assessments Team
Ocean-Atmosphere Processes Team
Data Assimilation and Predictions Team
Model Evaluation and Development Team
Tropical Dynamics Team

Water Cycle Branch

Coastal Processes Team
Hydrometeorological Processes Team
Observing Systems Team

Weather and Climate Physics Branch

Polar Observations and Processes Team
Boundary Layer Processes and Applications Team
Multiscale Interactions Team

FY09 PSD Staff Distribution

(Total=161)

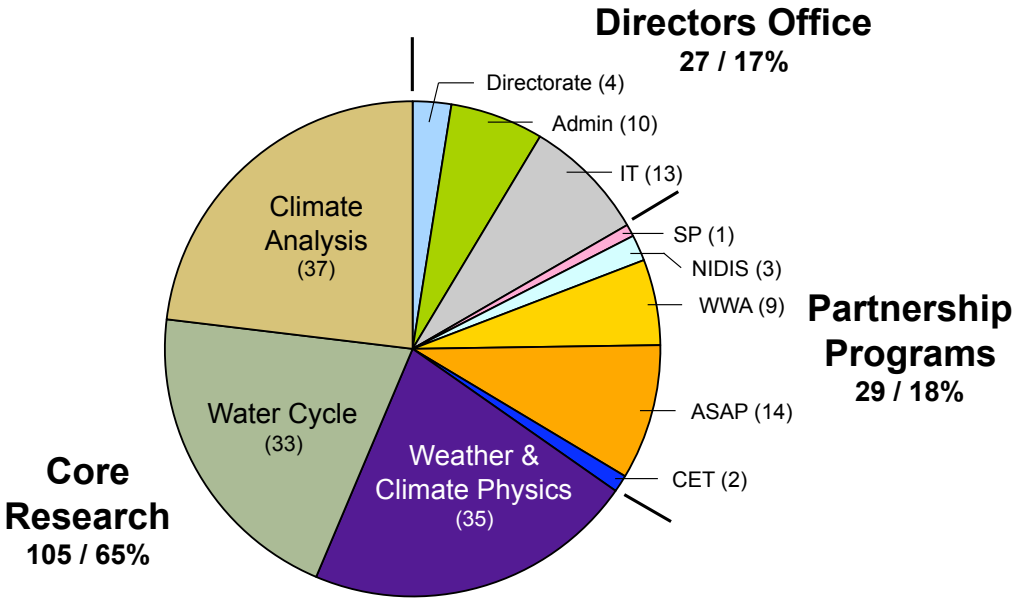

FY09 PSD Staff Degree Distribution and Functions

(Total=161)

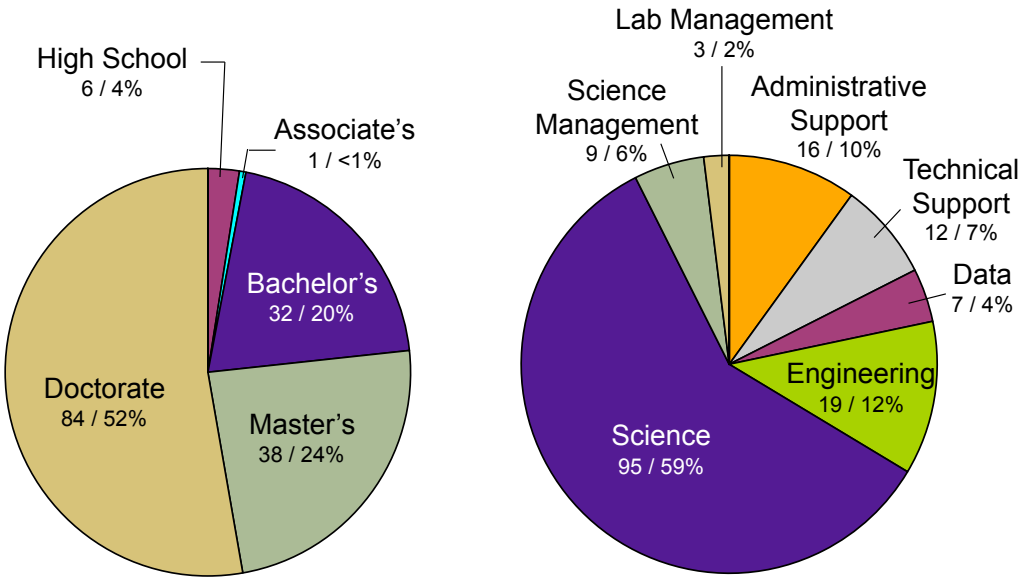

Cultivating the Next Generation of NOAA Scientists

Sample population includes (total = 34):
Cooperative Institute under 40 (13), Post Docs (6), Graduate Students (4), Summer Students (11)

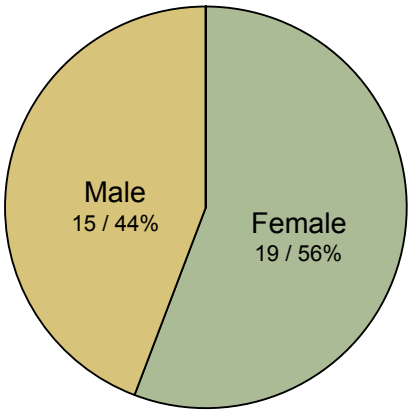

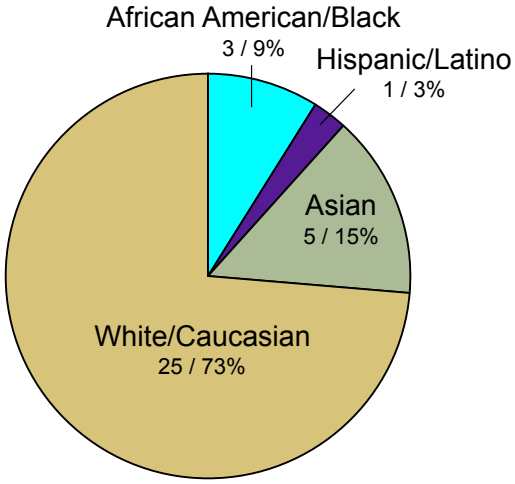

Summer student programs include: ISET (3), NOAA Hollings (2), SOARS (1), Contract College (2), Contract High School (3)

FY09 PSD Diversity

(Total=161)

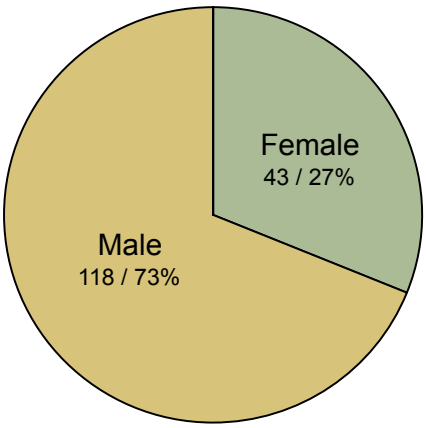

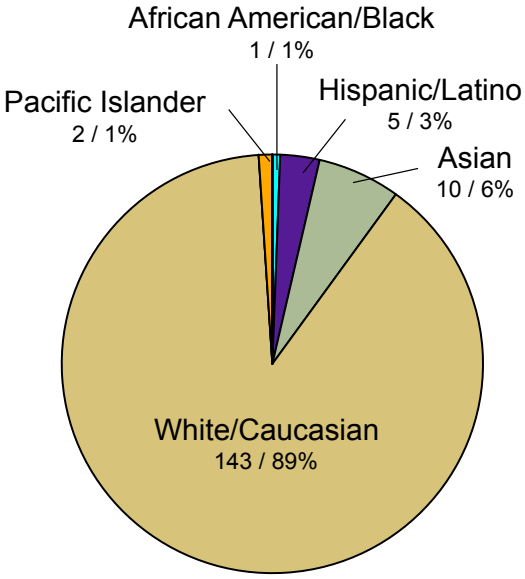

FY09 PSD Staff Age Distribution

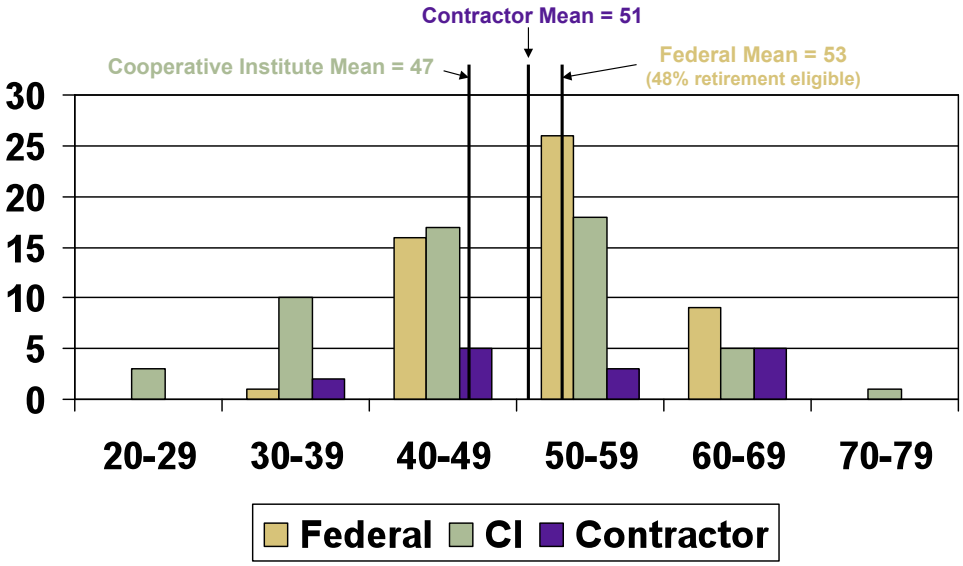

PSD Organization and Staff

Director's Office

Directorate

Neff, William (Director)
Dole, Randall (Deputy Director for Research)*
Lataitis, Richard (Deputy Director for Administration)
Schurman, Gloria (Administrative Support)

Budget and Administration Group

Gorton, Brian (Administrative Officer)

Davis, Jean
Lombardi, Rita
Madsen, Wendi
Novosel, Jo
Nyul, Angela
Otto, William
Sandberg, Christine
Frances Snow

Information Technology Group

Wilde, Nicholas (Senior IT Manager)

Falls, Michael
Estes, Eric (IT Security)

Systems Administration Team

Jesse, Rusty (Lead)
Healy, Kelly
McColl, Alex
McColl, Chesley
McInnes, Barry
Miller, Dan
Warnken, Ed

Web and Data Management Team

Smith, Cathy (Lead)
Hooper, Don
Keith, Gregory

Communication Group

DeLuisi, Barb

*Also coordinator of Research Partnership Programs

Research Partnership Programs

Dole, Randall (Deputy Director for Research)
Darby, Lisa

National Integrated Drought Information System (NIDIS)

Pulwarty, Roger (Director)
Verdin, James (Deputy Director)
McNutt, Chad

Western Water Assessment (WWA)

Udall, Brad (Director)
Averyt, Kristen (Deputy Director)

Alvord, Christina
Deems, Jeffery
Gordon, Eric
Guentchev, Galina
Lukas, Jeffrey
Mahoney, Kelly
Rangwala, Imitiaz
Ray, Andrea*
Wolter, Klaus*

Advanced Sensor Applications Program (ASAP)

Trujillo, Margarita (Manager), McClellan, Sandra (Coordinator)

Bedard, Alfred
Charnotskii, Mikhail
Fuks, Iosif
Godin, Oleg
Irisov, Vladimir
Naugolnykh, Konstantin
Nishiyama, Randall
Ostrovsky, Lev
Post, M.J.
Smirnov, Andre
Tatarskii, Valerian
Hill, Reginald

University of Colorado (CU)

Center for Environmental Technology (CET)

Gasiewski, Albin (Director)

Westwater, Ed

* Also member of Climate Analysis Branch

PSD Organization and Staff

Climate Analysis Branch

Webb, Robert (Chief)
Lucia Harrop (Administrative Support)
Herrli, Barbara (Administrative Support)
McAfee, Stephanie

Climate Dynamics Team

Sardeshmukh, Prashant (Lead)

Barsugli, Joseph, Compo, Gilbert, Lovejoy, Shaun, Newman, Matthew, Pegion, Kathy

Attribution and Assessments Team

Hoerling, Marty (Lead)

Diaz, Henry, Eischeid, Jon, Perlwitz, Judy, Quan, Xiao-Wei, Ray, Andrea, Wolter, Klaus, Xu, Taiyi, Zhang, Tao

Ocean-Atmosphere Processes Team

Alexander, Michael (Lead)

Capotondi, Antonietta, Scott, James, Sun, De-Zheng, Sun, Yan

Data Assimilation and Predictions Team

Whitaker, Jeffrey (Lead)

Bates, Gary, Hamill, Thomas, Pegion, Phillip

Model Evaluation and Development Team

Pincus, Robert (Lead), Hofmann, Patrick

Tropical Dynamics Team

Kiladis, George (Lead)

Allured, David, Liebmann, Brant, Leroux, Stephanie, Tulich, Stephan, Weickmann, Klaus, Zheng, Yangxing

Weather and Climate Physics Branch

Fairall, Christopher (Chief)
Wolfe, Daniel (Deputy Chief)
Martin, Karen (Administrative Support)

Polar Observations and Processes Team

Uttal, Taneil (Lead)

Chanders, Coy, Frisch, Shelby, Leuski, Vladimir, Moran, Kenneth, Persson, Ola, Solomon, Amy, Shupe, Matthew, Welsh, David, Wheeler, Cassie, Matsui, Nobuki

Boundary Layer Processes and Applications Team

Wilczak, James (Lead)

Bao, Jian-Wen, Bariteau, Ludovic, Bianco, Laura, Boylan, Patrick, Djalalova, Irina, Grachev, Andrey, Grell, Evelyn, Hare, Jeff, Hartten, Leslie, Lubker, Sandra, Michelson, Sara, Pezoa, Sergio, Woodruff, Scott

Multiscale Interactions Team

Penland, Cecile (Co-Lead); Voronovich, Alexander (Co-Lead)

Matrosova, Ludmilla, Ostashev, Vladimir, VanZandt, Thomas, Walsh, Edward, Zavorotny, Valery

Water Cycle Branch

Ralph, F. Martin (Chief)
King, Clark (Deputy Chief)*
Schiffbauer, Tina (Administrative Support)
Hughes, Mimi

Coastal Processes Team

White, Allen (Lead)

Clark, Wally, Coleman, Tim, Gottas, Daniel, Jackson, Darren, King, Clark, Neiman, Paul, Wick, Gary

Hydrometeorological Processes Team

Schneider, Tim (Lead)

Bartram, Bruce, Campbell, Carroll, Cifelli, Robert, Johnson, Lynn, Kingsmill, David, Matrosov, Sergey, Reinking, Roger, Stankov, B. Boba, Sukovich, Ellen, Williams, Christopher, Zamora, Robert

Observing Systems Team

Jordan, Jim (Lead)

Abbott, Scott, Ayers, Tom, Carter, David, Clark, Kurt, Costa, David, Hazen, David, Gibson, Janet, Johnston, Paul, Leach, Jesse

*Also member of Coastal Processes Team

FY09 PSD Publication Titles

1. Columnar water vapor retrievals from multifilter rotating shadowband radiometer data
2. Use of the Koppen-Trewartha climate classification to evaluate climatic refugia in statistically derived ecoregions for the people's republic of china
3. Comment on "Global warming and United States landfalling hurricanes"
4. Comment on " When will Lake Mead go dry?"
5. The performance of a global and mesoscale model over the central Arctic Ocean during late summer
6. Recent changes in freezing level heights in the tropics with implications for the deglacierization of high mountain regions.
7. Using dual-polarized radar and dual-frequency profiler for DSD characterization: A case study from Darwin, Australia.
8. Marine observations of old weather
9. Low-frequency variability in the Gulf of Alaska from coarse and eddy-permitting ocean models
10. Thermal footprints of whales
11. Comparison of ground-based millimeter-wave observations and simulations in the Arctic winter
12. NASA Cold Land Processes Experiment (CLPX 2002/03): Airborne remote sensing
13. Oceanic influences on recent continental warming
14. Arctic mixed-phase stratiform cloud properties from multiple years of surface-based measurements at two high-latitude locations
15. Sea surface temperature variability: Patterns and mechanisms
16. The seasonal atmospheric response to projected Arctic sea ice loss in the late twenty-first century
17. Ship observations of the tropical Pacific Ocean along the coast of South America
18. Numerical generation of stochastic differential equations in climate models
19. Investigation of the physical scaling of sea spray spume droplet production
20. A nonparametric approach for paleohydrologic reconstruction of annual streamflow ensembles
21. Atmosphere-ocean ozone exchange: A global modeling study of biogeochemical, atmospheric, and waterside turbulence dependencies
22. Climatology of surface meteorology, surface fluxes, cloud fraction, and radiative forcing over the southeast Pacific from buoy observations
23. Numerical simulations and observations of surface wave fields under an extreme tropical cyclone
24. Historical SAM variability. Part II: Twentieth-century variability and trends from reconstructions, observations, and the IPCC AR4 models
25. Intra-annual relationships between polar ozone and the SAM
26. Bistatic remote sensing
27. Emergence of deterministic Green's functions from noise generated by finite random sources
28. Retrieval of Green's functions of elastic waves from thermal fluctuations of fluid-solid systems
29. Stability of acoustic wave fronts propagating in anisotropic three-dimensional environments
30. Wave refraction at an interface: Snell's law versus Chapman's law
31. Variations in sea surface roughness induced by the 2004 Sumatra-Andaman tsunami
32. Evaluation of incremental improvements to quantitative precipitation estimates in complex terrain
33. Comments on "Sigma-point Kalman filter data assimilation methods for strongly nonlinear systems."
34. Alongfront variability of precipitation associated with a midlatitude frontal zone: TRMM observations and MM5 simulation
35. Imaging of atmospheric gravity waves in the stratosphere and upper mesosphere using satellite and ground-based observations over Australia during the TWPICE campaign
36. Spring and summertime diurnal surface ozone fluxes over the polar snow at Summit, Greenland.
37. Multiyear evaluations of a cloud model using ARM data
38. Distinct causes for two principal U.S. droughts of the 20th century
39. Hindcasts of tropical Atlantic SST gradient and South American precipitation: The influences of the

ENSO forcing and the Atlantic preconditioning
40. Improved multisensor approach to satellite-retrieved near-surface specific humidity observations
41. Dynamics of the west African monsoon. Part IV: Analysis of 25-90-day variability of convection and the role of the Indian monsoon
42. Evaluation and comparison of microphysical algorithms in WRF-ARW model simulations of atmospheric river events affecting the California coast
43. Convectively coupled equatorial waves
44. Application of MJO simulation diagnostics to climate models
45. Airflow and precipitation properties within the stratiform region of tropical storm Gabrielle during landfall
46. Intercomparison of model simulations of mixed-phase clouds observed during the ARM Mixed-Phase Arctic Cloud Experiment. I: Single-layer cloud
47. Ground-based passive microwave profiling during dynamic weather conditions
48. Evaluation of black carbon estimations in global aerosol models
49. Estimation of sea ice thickness distributions through the combination of snow depth and satellite laser altimetry data
50. Regional and local background ozone in Houston during Texas Air Quality Study 2006
51. Can we measure snow depth with GPS receivers?
52. Crossing thresholds in regional climate research: Synthesis of the IPCC expert meeting on regional impacts, adaptation, vulnerability, and mitigation
53. Origin of convectively coupled Kelvin waves over South America
54. Intraseasonal variability associated with summer precipitation over South America simulated by 14 IPCC AR4 coupled GCMs
55. Factors influencing the use of climate information by Colorado municipal water managers
56. The role of momentum transport in the motion of a quasi-idealized mesoscale convective system
57. A method to estimate vertically integrated amounts of cloud ice and liquid and mean rain rate in stratiform precipitation from radar and auxiliary data
58. Simultaneous estimates of cloud and rainfall parameters in the atmospheric vertical column above the Atmospheric Radiation Measurement Program Southern Great Plains site
59. Influence of multiple scattering on CloudSat measurements in snow: A model study
60. Assessing snowfall rates from X-band radar reflectivity measurements
61. Analysis and improvements of cloud models for propagation studies
62. An evaluation of real-time air quality forecasts and their urban emissions over eastern Texas during the summer of 2006 Second Texas Air Quality Study field study
63. Decadal prediction: Can it be skillful?
64. Intercomparison of model simulations of mixed-phase clouds observed during the ARM Mixed-Phase Arctic Cloud Experiment. II: Multilayer cloud
65. A water vapor flux tool for precipitation forecasting
66. Snowflake size spectra retrieved from a UHF vertical profiler
67. How important is air-sea coupling in ENSO and MJO evolution?
68. Transverse-longitudinal coherence function of a sound field for line-of-sight propagation in a turbulent atmosphere
69. Recent progress in acoustic travel-time tomography of the atmospheric surface layer
70. The problems of nonlinear acoustics which seem to be the most important and interesting today
71. A case study of the development of nocturnal slope flows in a wide open valley and associated air quality implications
72. Computational cost and accuracy in calculating three-dimensional radiative transfer: Results for new implementations of Monte Carlo and SHDOM
73. Water supply risk on the Colorado River: Can management mitigate?
74. Science and decision making: Water management and tree-ring data in the western United States
75. Review of FEWS NET biophysical monitoring requirements
76. Reconciling non-Gaussian climate statistics with linear dynamics
77. Stirring and mixing of liquids using acoustic radiation force

78. Rapid photochemical production of ozone at high concentrations in a rural site during winter
79. A U.S. CLIVAR project to assess and compare the responses of global climate models to drought-related SST forcing patterns: overview and results
80. Statistical representation of equatorial waves and tropical instability waves in the Pacific Ocean
81. A vision for climate services in NOAA
82. Investigation of microphysical parameterizations of snow and ice in Arctic clouds during M-PACE through model-observation comparisons
83. Variability of graupel and snow observed in tropical oceanic convection by aircraft during TRMM KWAJEX
84. Tropical water vapor and cloud feedbacks in climate models: A further assessment using coupled simulations
85. A global view of air-sea thermal coupling and related non-Gaussian SST variability
86. A field study of reflectivity and Z-R relations using vertically pointing radars and disdrometers
87. Atmospheric forcing of Fram Strait sea ice export
88. A national interagency water plan
89. Coherence function of a sound field in an oceanic waveguide with horizontally isotropic statistics
90. Midlatitude excitation of tropical variability in the Pacific: The role of thermodynamic coupling and seasonality
91. MJO simulation diagnostics
92. A comparison of the hybrid and EnSRF analysis schemes in the presence of model errors due to unresolved scales
93. Attribution of the seasonality and regionality in climate trends over the United States during 1950–2000
94. Wavelet analysis and filtering to identify dominant orientations of permeability anisotropy
95. Effect of zonal asymmetries in stratospheric ozone on simulated southern hemisphere climate trends
96. The tropical Madden-Julian oscillation and the global wind oscillation
97. A comparison of variational and ensemble-based data assimilation systems for reanalysis of sparse observations
98. Analysis of regional meteorology and surface ozone during the TexAQS II field program and an evaluation of the NMM-CMAQ and WRF-Chem air quality models
99. Raindrop size distribution variability estimated using ensemble statistics
100. Quasi-wavelet formulations of turbulence and other random fields with correlated properties
101. Moment-screen method for sound propagation in a refractive medium with random scattering
102. Quasi-wavelet formulations of turbulence and wave scattering
103. Measuring storm surge with an airborne wide-swath radar altimeter
104. Response of ENSO and the mean state of the tropical Pacific to extratropical cooling and warm ing: A study using the IAP coupled model
105. Modulation instability: The beginning
106. The role of boundary layer processes in limiting PV homogenization.
107. Atmospheric inverse estimates of methane emissions from central California.
108. Ocean heat transport in simple ocean data assimilation: Structure and mechanisms
109. Foreword to the special issue on unmanned airborne vehicle (UAV) sensing systems for earth observations
110. Stratocumulus cloud-top height estimates and their climatic implications

Seasonal Forecasting of Thermal Stress Conducive to Mass Coral Bleaching Events

C. Penland[1], L. Matrosova[2], R.S. Webb[1], R.S. Pulwarty[1], G. Liu[3], C.M. Eakin[4], S. Lynds[2], T.R.L. Christensen[3], S.F. Heron[3], J.A. Morgan[3], B.A.A. Parker[3], W.J. Skirving[3], A.E. Strong[4]

[1]NOAA Earth System Research Laboratory, Boulder, CO; [2]CIRES, University of Colorado, Boulder, CO; [3]IMSG/NOAA Coral Reef Watch, Silver Spring, MD; [4]NOAA Coral Reef Watch, Silver Spring, MD

Introduction: Coral bleaching has been increasing in both frequency and severity over the past decades. NOAA Coral Reef Watch (CRW) began providing global seasonal outlooks of thermal stress conducive to coral bleaching in July 2008. Combined with CRW's near-real-time satellite monitoring of thermal stress, this outlook has significantly improved management of coral reef ecosystems through advanced warning of bleaching conditions. The outlook system was developed jointly by CRW and Earth System Research Laboratory (ESRL). The bleaching outlook product is intended to provide large-scale patterns of potential bleaching (not for any particular reef location), thus enabling managers and scientists to prepare.

2009 Dec 01 NOAA Coral Reef Watch Coral Bleaching Thermal Stress Outlook for Dec–Mar 2010

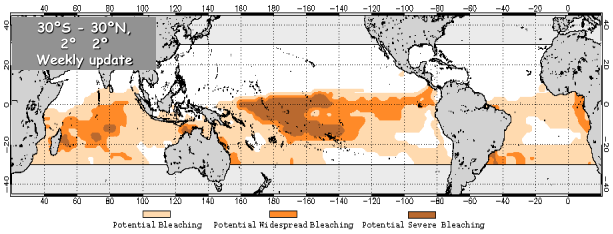

CRW Satellite Near-Real-Time Coral Bleaching Monitoring Products (Operational, twice-weekly, 0.5-degree (~50km), Liu *et al.* 2006)

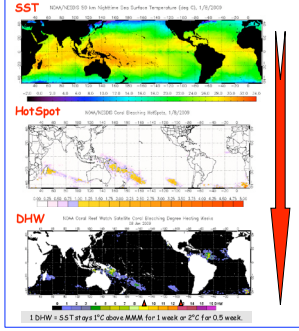

Bleaching HotSpot intensity of thermal stress as the difference between the observed SST at a grid point and the climatologically averaged temperature for the warmest month (maximum monthly mean).

Bleaching Degree Heating Weeks (DHW) intensity and duration of thermal stress associated with bleaching occurrence and intensity, accumulated HotSpot values ≥1.0 °C during prior 12 weeks.

▲ DHW >4 °C-weeks significant bleaching likely; ≥8 °C-weeks widespread severe bleaching and mortality likely.

References:
Liu G, Strong AE, Skirving W, Arzayus LF (2006) Overview of NOAA Coral Reef Watch Program's near-real time global satellite coral bleaching monitoring activities. *Proc. 10th Int Coral Reef Symp, Okinawa, Japan*. 1783-1793
Penland C, Matrosova L (1998) Prediction of tropical Atlantic sea surface temperatures using linear inverse modeling. *J Climate* 11: 483-496
Reynolds RW, Rayner NA, Smith TM, Stokes DC, Wang W (2002) An improved in situ and satellite SST analysis for climate. *J Climate* 16: 1609-25

Bleaching Outlook System

(1) Weekly SST Forecast (leadtime of 1 to 18 weeks). Weekly SST predictions produced by the ESRL Linear Inverse Model (Penland and Matrosova, 1998). Weekly 1°x1° Reynolds and Smith Optimum Interpolation SST data (Reynolds *et al.* 2002) used to train and initialize model.

⇩

(2) Weekly Thermal Stress Forecast (Bleaching HotSpot & Degree Heating Week). Algorithm for deriving thermal stress forecasts from SST predictions modified from CRW operational near-real-time satellite thermal stress monitoring algorithm.

⇩

(3) Weekly Thermal Stress Bleaching Outlook. Potential thermal stress is categorized into three levels based on values of HotSpot and Degree Heating Weeks.

⇩

(4) Seasonal Thermal Stress Bleaching Outlook. Seasonal outlook at each 2°x2° grid cell equals highest potential thermal stress level among all weekly outlooks during the 4-month prediction period.

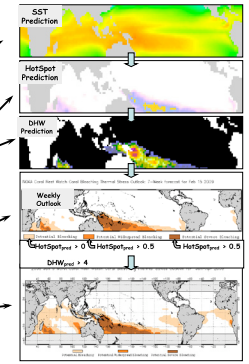

Sample Weekly Prediction for February 12-18, 2009 (based on Weekly OISST ending on December 31, 2008)

coralreefwatch.noaa.gov

Comparison of Seasonal Bleaching Outlooks and CRW Satellite Bleaching Stress Estimates

2001-2009 Austral Bleaching Season (Jan-Apr) 2001-2009 Boreal Bleaching Season (July-Oct)

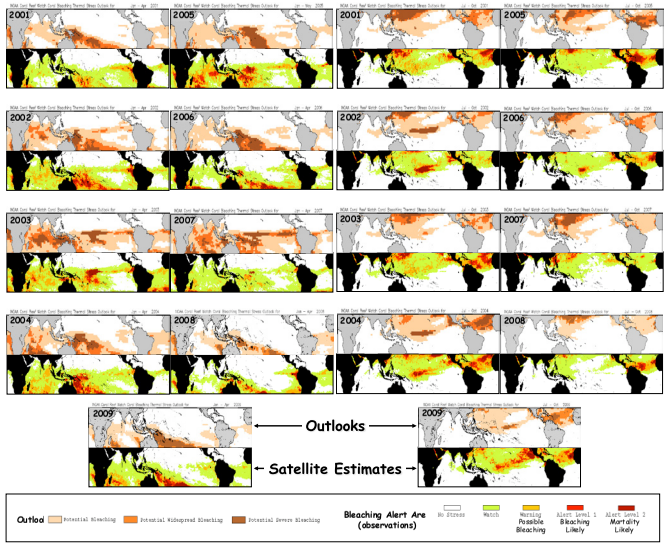

Discussion and Results:

- Accuracy of bleaching outlooks are assessed for 2001-2009 boreal and austral bleaching seasons by comparing seasonal outlooks with CRW satellite bleaching stress estimates.
- Outlooks generally match observed HotSpot and DHW.
- Outlooks perform best in the Caribbean & Great Barrier Reef
- Outlooks do not perform as well in the northwestern Hawaiian Islands.
- Analyses of weekly predictions (not shown) indicate the prediction system captures timing of development and dissipation of thermal stress during mass coral bleaching events.
- Over-predicted thermal stress in the Caribbean for the 2009 bleaching season, possibly due to persistence of strong zonal winds and lack of the extra-tropical SSTs forecasts.

Future Work: In addition to evaluating and improving the current thermal stress bleaching outlook product, next steps include developing an outlook product based on the NOAA NCEP Climate Forecast System (CFS) model.

NOAA CORAL REEF CONSERVATION PROGRAM · Earth System Research Laboratory Physical Sciences Division · IMSG I.M. Systems Group, Inc. · CIRES

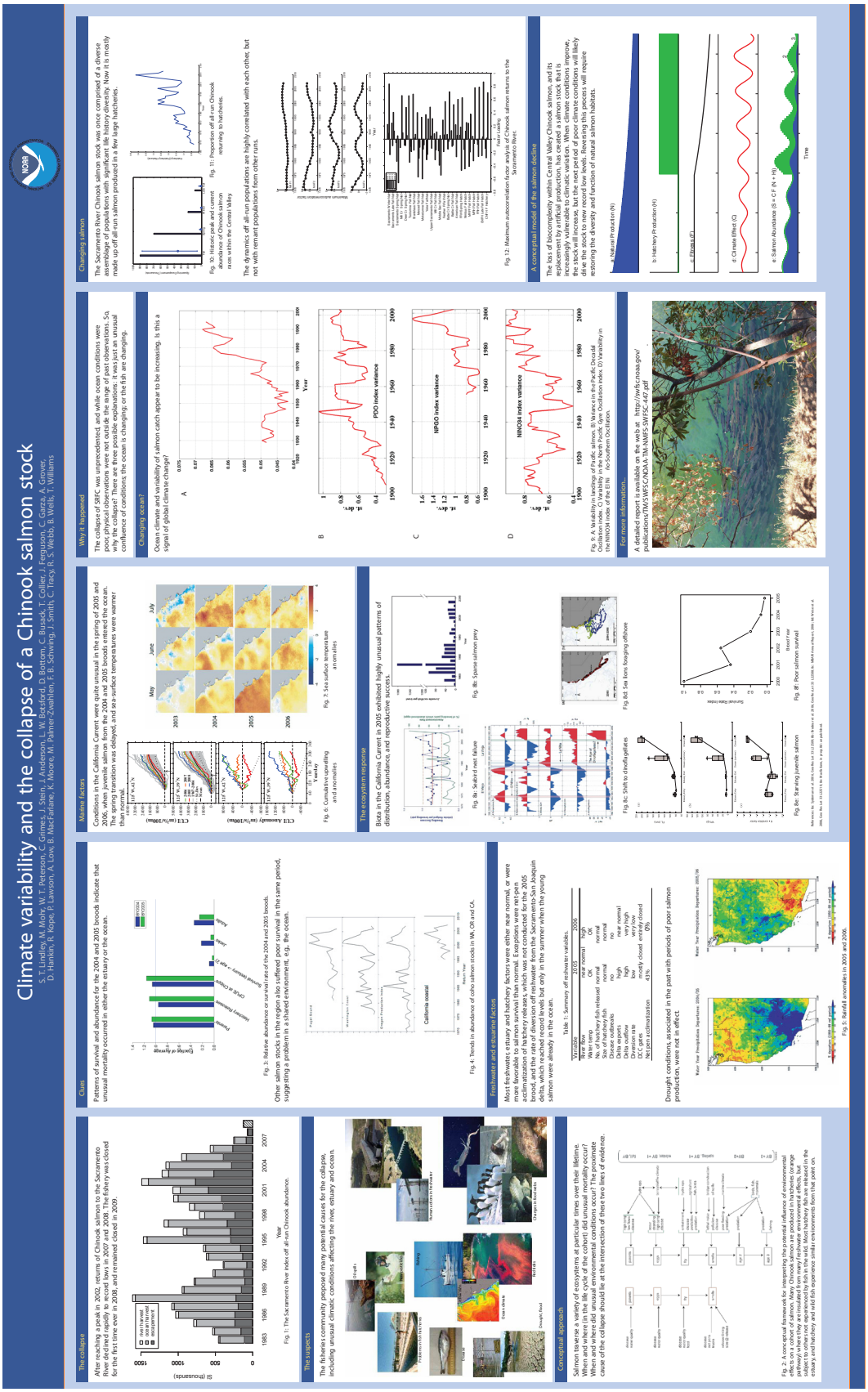
Climate variability and the collapse of a Chinook salmon stock
S.T. Lindley, M. Mohr, W. T. Peterson, C. Grimes, J. Stein, K. Anderson, J. Wells, J. Hobday, D. Bellier, D. Huff, J. Eptesam, C. Garza, A. Grover, D. Hankin, R. Kope, P. Lawson, A. Low, B. MacFarlane, K. Moore, M. Palmer-Zwahlen, F. B. Schwing, J. Smith, C. Tracy, R. Webb, B. Wells, T. Williams
The collapse
After reaching a peak in 2002, returns of Chinook salmon to the Sacramento River declined rapidly to record lows in 2007 and 2008. The fishery was closed for the first time ever in 2008, and remained closed in 2009.
Fig. 1: The Sacramento River index of all-run Chinook abundance.
Clues
Patterns of survival and abundance for the 2004 and 2005 broods indicate that unusual mortality occurred in either the estuary or the ocean.
Fig. 3: Relative abundance or survival rates of the 2004 and 2005 broods.
Other salmon stocks in the region also suffered poor survival in the same period, suggesting a problem in a shared environment, e.g., the ocean.
Fig. 4: Trends in abundance of coho salmon stocks in WA, OR and CA.
Marine factors
Conditions in the California Current were quite unusual in the spring of 2005 and 2006, when juvenile salmon from the 2004 and 2005 broods entered the ocean. The spring transition was delayed, and sea-surface temperatures were warmer than normal.
Fig. 6: Cumulative upwelling and anomalies
Fig. 7: Sea surface temperature anomalies
Why it happened
The collapse of SRFC was unprecedented, and while ocean conditions were poor, physical observations were not outside the range of past observations. So, why the collapse? There are three possible explanations: it was just an unusual confluence of conditions; the ocean is changing; or the fish are changing.
Changing ocean?
Ocean climate and variability of salmon catch appear to be increasing. Is this a signal of global climate change?
Fig. 9: A: Variability in landings of Pacific salmon, B: Variance in the Pacific Decadal Oscillation Index, C: Variance in the North Pacific Gyre Oscillation Index, D: Variability in the NINO34 index of the El Ni ño-Southern Oscillation.
For more information:
A detailed report is available on the web at: http://nwfsc.noaa.gov/publications/TM/SWFSC/NOAA-TM-NMFS-SWFSC-447.pdf
Changing salmon
The Sacramento River Chinook salmon stock was once comprised of a diverse assemblage of populations with significant life history diversity. Now it is mostly made up of all-run salmon produced in a few large hatcheries.
Fig. 10: Historic peak and current abundance of Chinook salmon races within the Central Valley
Fig. 11: Proportion of all-run Chinook returning to hatcheries.
The dynamics of all-run populations are highly correlated with each other, but not with remnant populations from other runs.
Fig. 12: Maximum autocorrelation factor analysis of Chinook salmon returns to the Sacramento River.
A conceptual model of the salmon lifecycle
The loss of biocomplexity within Central Valley Chinook salmon, and its replacement by artificial production, has created a salmon stock that is increasingly vulnerable to climate variability. If habitat conditions improve, the stock will increase, but the next period of poor climate conditions will likely drive the stock to new record low levels. Reversing this process will require restoring the diversity and function of natural salmon habitats.
a. Natural Production (N)
b. Hatchery Production (H)
c. Fitness (F)
d. Climate Effect (C)
e. Salmon Abundance (S = C F (R + H))
Time
Freshwater and estuarine factors
Most freshwater, estuary and hatchery factors were either near normal, or were more favorable to salmon survival than normal. Exceptions were net-pen acclimatization of hatchery releases, which was not conducted for the 2005 brood, and the quality of estuarine habitat in the Sacramento-San Joaquin delta, which reached record levels but only in the summer when the young salmon were already in the ocean.
Table 1: Summary of freshwater variables.
Variable 2005 2006
Water flow not normal high
Water temp OK OK
No. of hatchery fish released normal
Size of hatchery fish normal normal
Disease in hatcheries low low
Delta exports high near normal
Delta flow high very high
Diversion rate low very low
DCC gates mostly closed entirely closed
Net pen acclimatization 41% 0%
Droughts conditions, associated in the past with periods of poor salmon production, were not in effect.
The ecosystem response
Biota in the California Current in 2005 exhibited highly unusual patterns of distribution, abundance, and reproductive success.
Fig. 8a: Sold red failure
Fig. 8b: Spawn salmon prey
Fig. 8c: Shift to chrodogadiles
Fig. 8d: Sea lions foraging offshore
Fig. 8e: Starving juvenile salmon
Fig. 8f: Poor salmon survival
The suspects
The fisheries community proposed many potential causes for the collapse, including unusual climatic conditions affecting the river, estuary and ocean.
Conceptual approach
Salmon traverse a variety of ecosystems at particular times over their lifetime. When and where did unusual environmental conditions occur? The proximate cause of the collapse should lie at the intersection of these two lines of evidence.
Fig. 2: A conceptual framework for interpreting the potential influence of environmental effects on a cohort of salmon. Many Chinook salmon are produced in hatcheries (orange pathway) where they are insulated from many freshwater environmental effects, but experience hatchery effects. Wild fish must survive and grow in the river, in the estuary and hatchery and wild fish experience similar environments from that point on.
Fig. 5: Rainfall anomalies in 2005 and 2006.

The Climate Response to 2007 Arctic Sea Ice Loss

Depleted Arctic Sea Ice

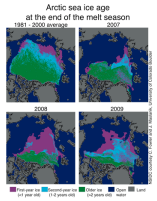

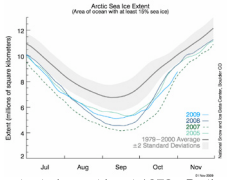

Arctic sea ice in 2007 reached its lowest extent since at least 1978. By the end of the melt-season in September, sea ice suffered a -39% areal decline, with an unusual exposure of a vast expanse of the Arctic Ocean occurring poleward of the Russian and western North American coasts (top figures, from NSIDC)

Observed Arctic Warming

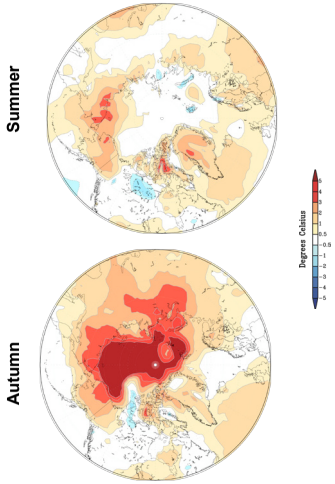

Most of the Arctic experienced high surface temperatures in 2007, especially over the Arctic Ocean in Autumn in areas where sea ice vanished. Considerable warmth also occurred over the Arctic tundra. The recent high latitude warming is consistent with the emergence of a surface-based Arctic amplification (Serreze et al. 2009).

Observed Data: Summer (June-July-August) and Autumn (September-October-November) surface air temperature is based on the Hadley Center's CRTUv3 and NASA analyses over land, and on the NCEP-NCAR Reanalysis over the Arctic Ocean. Reference period is 1971-2000.

Assessing Impacts of 2007 Arctic Sea Ice

Q1: What was the impact of 2007 sea ice conditions on Arctic surface temperature?
Sea ice loss explains virtually all of the autumnal warming over the Arctic Ocean during 2007. Sea ice impacts on temperature are confined mostly poleward of 60°N.

Q2: What was the seasonality of the sea ice impacts during 2007?
The greatest sea-ice induced warming occurred in the Autumn and early Winter.

***Q3:* How did the Arctic tundra respond to 2007 sea ice relative to the Arctic Ocean?**
Autumn Arctic tundra (land poleward of 60°N) surface temperatures warmed by +1.3°C due to sea ice forcing compared to a +3.9°C warming averaged over the Arctic Ocean. Sea ice exerted little or no impact on land temperatures equatorward of 60°N.

Simulated Arctic Warming

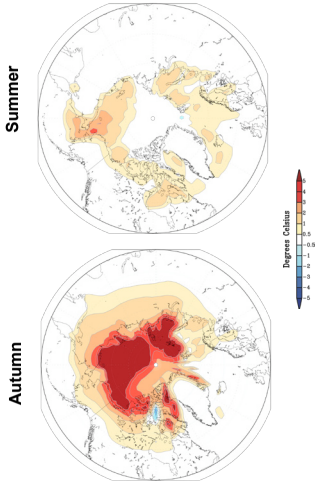

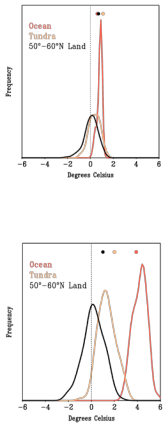

To address the above questions, atmospheric GCMs were subjected to the 2007 monthly global SSTs and sea ice, while a parallel suite used the same SSTs but climatological sea ice. Their difference evaluates the 2007 sea ice impacts. Also shown are probability distribution functions, based on 150 runs, of surface temperature for three regions (observed values shown by dots):
a) Arctic Ocean poleward of 65°N, b) Arctic tundra poleward of 60°N, c) land between 50°-60°N

Model Data: Three models were used: NCEP's GFS, GFDL's AM2.1, and NCAR's CCM3.
A 50-member ensemble was conducted with each model, and for each of the two boundary forcings

Martin Hoerling, Judith Perlwitz, Jon Eischeid, Xiao-Wei Quan, TaiYi Xu, and Arun Kumar[1]: ***NOAA Earth System Research Laboratory and [1]NOAA NCEP***

Attribution of Evolving North American Climate Conditions

Judith Perlwitz[1,2], Martin Hoerling[1], Jon Eischeid[1,2], Taiyi Xu[1,2] and Arun Kumar[3]
[1]NOAA/ESRL/PSD, [2]CIRES/CU and [3]NOAA/NCEP/NWS

1970-2007 Trend

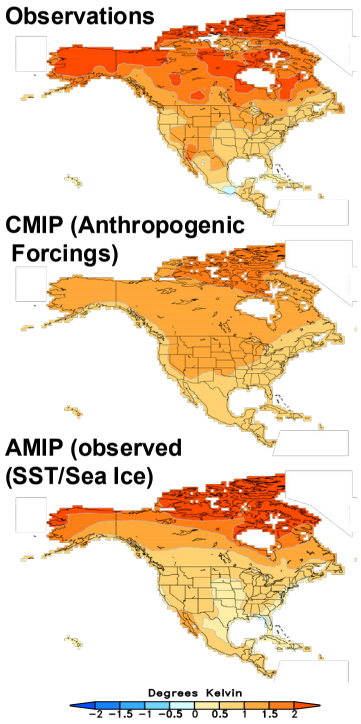

Q: What caused North American warming since 1970?

A: Model simulations indicate that most of the observed warming was due to anthropogenic forcing. The physical process of continental warming was via the influence of SST and sea ice changes.

2008 Anomalies

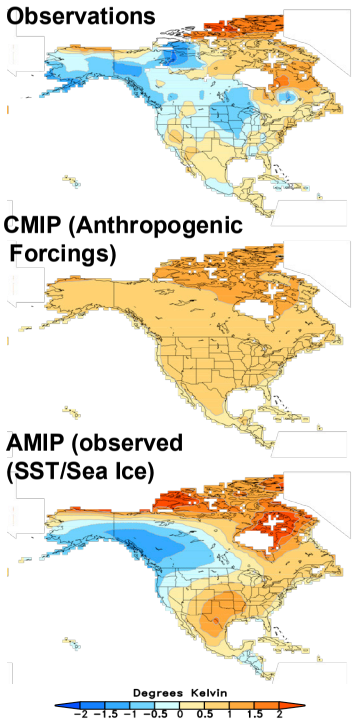

Q: Why did the warming not continue in 2008?

A: Model simulations indicate that 2008 coolness was caused by a strong bout of naturally-induced cooling. This resulted from the continents sensitivity to unusually cold SSTs in the tropical Pacific.

Appraisal of 2008 Climate Conditions

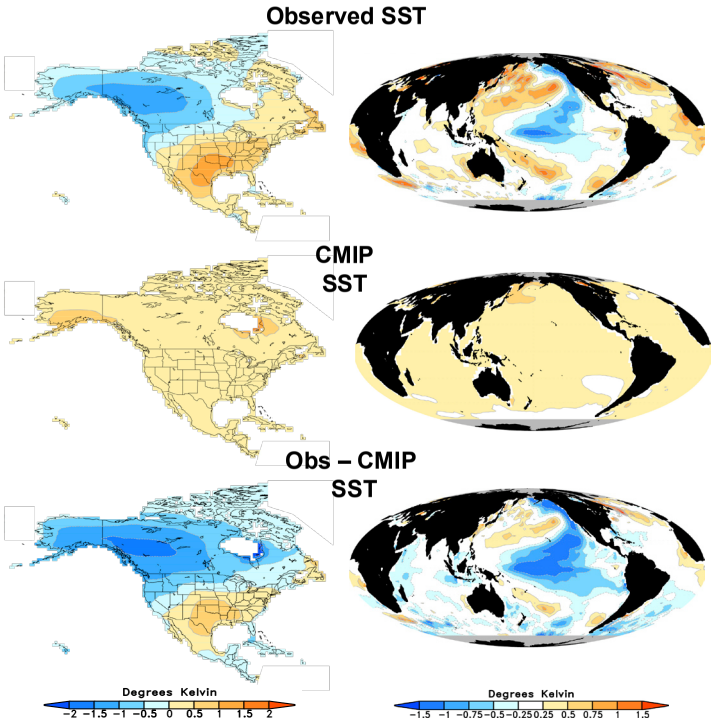

Q: What was the natural versus anthropogenic impact on 2008 North American temperatures?

A: AGCMs forced by estimates of the natural and anthropogenic components of 2008 SST conditions indicate that the warmth induced by the latter was overwhelmed by the coolness induced by the natural state of SSTs. 2008 NA temperatures would have been considerably cooler in the absence of anthropogenic forcing.

PSD Interactive Data Analysis and Plotting Web Pages:
http://www.esrl.noaa.gov/psd/

PSD makes a selection of Web-based tools available that allow users to easily plot data, as well to quickly test climate/weather hypotheses without having to download files or install libraries and code.

Data Analysis Web Pages

Web-based data products at PSD include compositing tools (average hourly, daily and monthly data), plotting pages, timeseries extraction, Hovmollers, vertical cross-sections, radar plots, and accumulation plots. On some pages, users can upload their own data for use on the pages. Pages are designed to be easy to use with interfaces geared towards the analysis.

Users and Statistics

Users of PSD's Web pages include NOAA and the NWS offices, researchers, graduate students, resource managers, energy companies, farmers, skiing resorts, teachers, and weather enthusiasts, among many others. PSD gets about **1.5 million web hits a month.**

Some Datasets Available at PSD

- **Reanalysis Datasets**: NCEP/NCAR I, NARR, 20th Century, NCEP/DOE II…
- **Analysis**: NCEP Operational…
- **Gridded Precipitation**: CMAP, GPCP, GPCC…
- **SST**: ICOADS, Kaplan SST, NOAA OI…
- **Instrumental**: Wind Profiler, Radar…
- **Cruise Data**: Flux, profiler, ceilometer,…
- **Model Output**: GFS, MJO models
- **Satellite**: SST, Heat Fluxes…

Data is generally available via ftp. Some data can be accessed via OPeNDAP. Instrumental data is accessible via a MySQL database. Gridded data is stored in CF-compliant NetCDF files.

PSD's Web Team

Barb DeLuisi, Don Hooper, Greg Keith, Cathy Smith, Tim Coleman, Dan Gottas (and many other contributors)

Gridded Climate Datasets

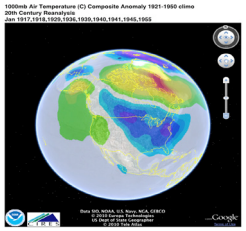

Near Surface Air Temperature from the 20th Century Reanalysis is plotted for low NAO wintertime years and displayed in Google Earth on the web.
http://www.esrl.noaa./gov/psd/data/20thC_Rean/

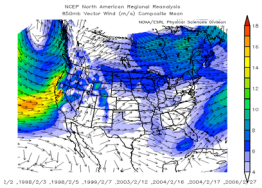

Vector Wind is composited for days with high "Atmospheric River" activity over central California.
http://www.esrl.noaa.gov/psd/data/narr/

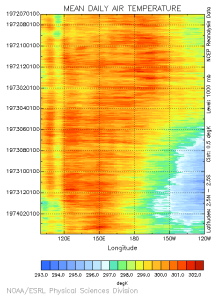

A Hovmoller (longitude by time) plot of surface air temperature shows the El Niño of 1973 transitioning to the strong La Niña of 1974 using the NCEP Reanalysis.
http://www.esrl.noaa.gov/psd/map/time_plot/

Climate Timeseries

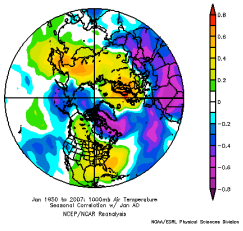

A linear correlation of the wintertime AO timeseries with Air Temperature from the NCEP Reanalysis.
http://www.esrl.noaa./gov/psd/data/correlation/

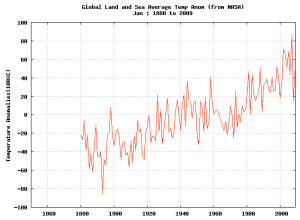

A plot of the January globally averaged surface temperature from 1880 to the present from the GISS Temperature dataset:
http://www.esrl.noaa.gov/psd/data/climateindices/

Forecasts

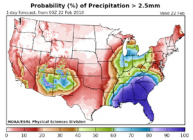

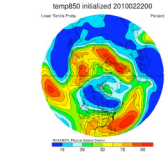

The NCEP ensemble forecast model output is downscaled using the NARR data in the first figure and is shown as tercile probability map in the 2nd figure:
http://www.esrl.noaa.gov/psd/forecasts/reforecasts/

Instrumental Data

Data browser for the BAO observatory site in Erie, Colorado: Users can extract different variables, timescale and dates using a simple interface.
http://www.esrl.noaa.gov/psd/technology/bao/

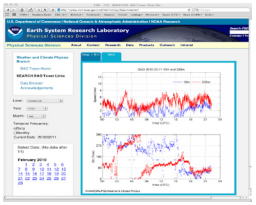

Trajectory Tool: Plots trajectories from data collected during Texas Air Quality Project (TEXAQS).
http://www.esrl.noaa.gov/psd/programs/texaqs/2006/

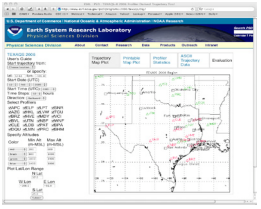

Wind Profiler Page: Pages display up-to-date data from the ensemble of profiler sites. Raw values can also be downloaded. http://www.esrl.noaa.gov/psd/data/psd/obs/

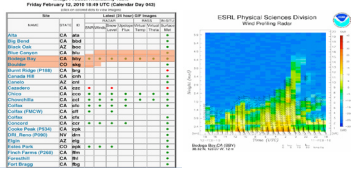

The Impact of Stratospheric Ozone Hole Recovery on Antarctic Climate

Judith Perlwitz [1,2], Steven Pawson [3], Ryan Fogt [2], Eric Nielsen[4], William Neff [2],

(1) CIRES, University of Colorado, Boulder, CO; (2) NOAA-ESRL Physical Sciences Division, Boulder, CO;

(3) NASA Goddard Space Flight Center, Greenbelt, MD; (4) Science Systems and Application, INC, Landham, MD

Introduction

- Model experiments have revealed that both stratospheric polar ozone depletion and anthropogenic increase of greenhouse gases (GHG) have contributed to the observed increase of summertime tropospheric westerlies in the Southern Hemisphere (SH) , but with ozone influence dominating.
- As the stratospheric halogen loading decreases in the future, ozone is expected to return to higher values, with the disappearance of the Antarctic ozone hole. The relative contributions of ozone hole recovery and GHG increases on the SH circulation changes during the 21st century (C21) are not well quantified.
- We estimate the impact of ozone recovery on SH polar climate using the coupled chemistry climate model GEOS-CCM.
- We will contrast the impacts of polar ozone depletion in the 20th century and recovery in the 21st century on the circulation, and relate the results to those from IPCC AR4 C21 simulations.

Experiments

Experiment	Time Period	SST	Halogens	Greenhouse Gases
P-1	1950-2004	Had1SST	Observed	Observed
P-2	1951-2004	Had1SST	Observed	Observed
P-Cl1960	1960-2004	Had1SST	Chlorine fixed at 1960 values	Observed with chlorine fixed at 1960 values
C21-1	1996-2099	HadGEM1	WMO Baseline scenario Ab	IPCC/GHG scenario A1b (medium)
C21-2	2000-2099	CCSM3.0	WMO Baseline scenario Ab	IPCC/GHG scenario A1b (medium)
C21-Cl1960	2001-2099	CCSM3.0	Chlorine fixed at 1960 values	IPCC/GHG scenario A1b (medium), with chlorine fixed at 1960 values

70-hPa Minimum Zonal Mean Ozone over Southern Hemisphere Polar Cap Area (90°S-60°S)

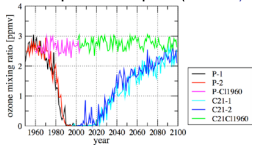

Ozone-Antarctic Climate: Past Changes 1999 minus 1969

Atmospheric Changes

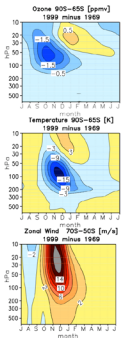

Changes in Near Surface Pressure

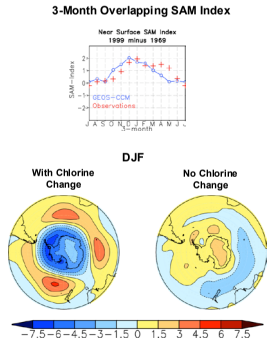

Ozone-Antarctic Climate: 21st Century Changes 2094 minus 2006

With Chlorine change / No Chlorine change

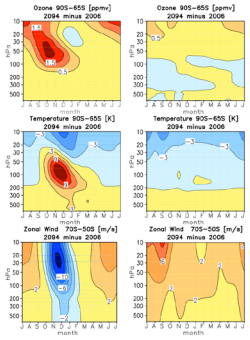

Changes in Near Surface Pressure

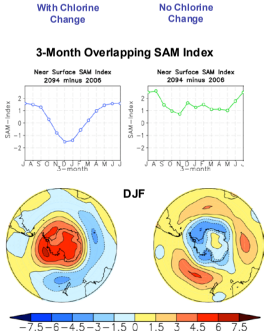

Comparison with AR4 Models 21st Century Changes 2094 minus 2006

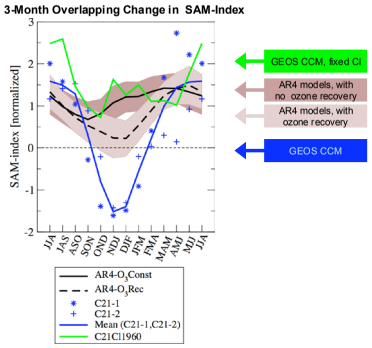

Summary and Conclusions

- In the GEOS CCM, ozone hole causes substantial seasonal circulation changes in accord with prior observations and model based studies
- This signal diminishes as ozone recovers through the 21st Century, even as GHGs continue to increase
- Ozone change signals swamp the impact of GHG increases in the 1970-2100 period
- AR4 ensembles suggest this same impact can be captured in climate models (with no stratosphere and imposed ozone change), though damped
- Need to test this in a fully coupled ocean-atmosphere-chemistry model.

More Information:

Perlwitz, J., S. Pawson, R. L. Fogt, J. E. Nielsen, and W. D. Neff (2008), Impact of stratospheric ozone hole recovery on Antarctic climate, Geophys. Res. Lett., 35, L08714, doi: 10.1029/2008GL033317

Distinguishing the roles of natural and anthropogenically forced decadal climate variability: Implications for prediction

ESRL/PSD's contribution to The US CLIVAR Decadal Predictability Working Group
Amy Solomon and Matt Newman

Objectives of The US CLIVAR Decadal Predictability Working Group:

✧*To define a framework to distinguish natural variability from anthropogenically forced variability on decadal time scales for the purpose of assessing predictability of decadal-scale climate variations.*

✧*Work towards better understanding of decadal variability and predictability through metrics that can be used as a strategy to assess and validate decadal climate prediction simulations.*

Scientific Focus #1:

Does the response to external forcing project onto or physically interact with natural climate variability?

Climate model simulations of the 20th Century indicate that the climate change signal may project on natural variability--Dominant pattern fluctuates on decadal timescales with an amplitude that varies from model to model and is larger than observations. In addition, note the differences in spatial patterns across models.

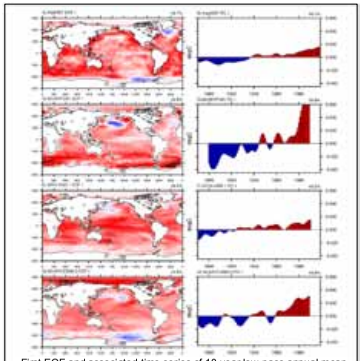

First EOF and associated time series of 10-year low-pass annual mean sea surface temperature from observations and three 20th Century simulations for years 1890-1999. (A,B) HadISST (C,D) NCAR/PCM1 (E,F) GFDL/CM2.1 (G,H) NCAR/CCSM3.0. From Solomon et al. (2010).

Scientific Focus #2:

Given that on regional scales the magnitude of natural decadal variations may rival that of anthropogenically forced climate change, how do we quantify predictable variability in decadal forecasts?

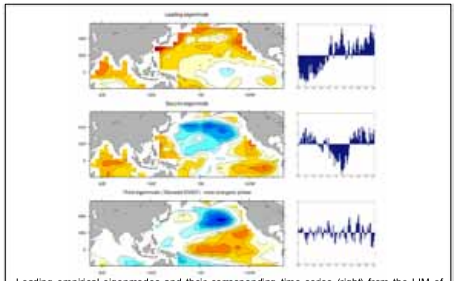

Leading empirical eigenmodes and their corresponding time series (right) from the LIM of annual-mean HadISST SST anomalies Red (blue) shading indicates positive (negative) values. a) Leading eigenmode, stationary with decay time of 13 yrs. b) Second eigenmode, stationary with decay time of 6.4 yrs. c) Most energetic phase of third ("decadal ENSO") eigenmode, propagating with period 16 yrs and decay time of 2.1 yrs. From Newman (2010)

Scientific Focus #3:

Do we have robust estimates of observed (or simulated) decadal trends?

Different mechanisms disagree on the expected sign of change in the zonal SST gradient in tropical in response to anthropogenic forcing. The observational record does little to clarify the situation, as trends in different observed SST records differ in even their sign, motivating further study with focused model experiments.

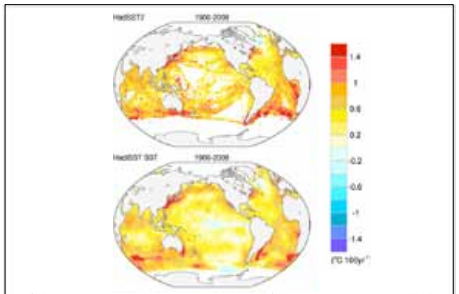

20th Century sea surface temperature trends (C 100 yr^{-1}) from the un-interpolated HadSST2 (top) and reconstructed HadISST (bottom) based on monthly anomalies during 1900-2008. From Deser et al. (2010).

Scientific Focus #4:

To develop a suite of metrics to assess CMIP5 near-term climate forecasts

For the purpose of:
➙Assessing the expectations for added regional climate information and skill achievable from initialized decadal predictions
➙Identifying physical processes or modes of variability that are important to the decadal prediction and predictability problem and whether their relevance may evolve with time
➙Attributing regional changes in the current climate to natural climate variations or anthropogenic forcing

An example of a metric to isolate externally-forced variability that is predictable on decadal timescales and can be used to assess the response of climate models to external forcing

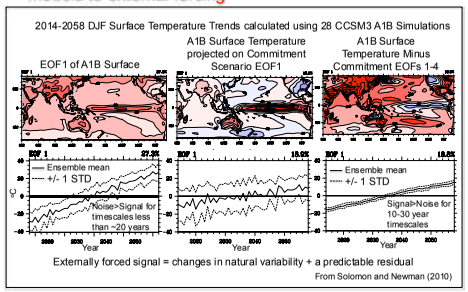

US CLIVAR Decadal Predictability Working Group Members:
Amy Solomon (co-chair,U. Colorado/NOAA),Lisa Goddard (co-chair,IRI/Columbia U.),Arun Kumar (co-chair,NOAA),George Boer(CCCMA), James Carton(U. Maryland),Tom Delworth(NOAA),Clara Deser(NCAR), Ichiro Fukumori(NASA),Arthur M. Greene(IRI),Gabriele Hegerl(U. Edinburgh),Ben Kirtman(U. Miami),Yochanan Kushnir(Columbia U.), Jerry Meehl(NCAR),Matthew Newman(U. Colorado/NOAA), Doug Smith(UKMET),Timothy Stockdale(ECMWF),Dan Vimont(U. Wisconsin)

see http://www.usclivar.org/wgdp.php for more details

References:

Deser, C., A.S. Phillips, and M.A.Alexander, 2010: A re-assessment of 20th Century sea surface temperature trends over the tropical Pacific. *GRL*, under review.
Newman, M., 2007: Interannual to decadal predictability of tropical and North Pacific sea surface temperatures. *J. Climate*, **20**, 2333–2356.
Solomon, A. and Coauthors, 2010: Distinguishing the roles of natural and anthropogenically forced decadal climate variability: Implications for prediction. *BAMS*, under review.

Using reforecasts to improve probabilistic weather predictions

Tom Hamill, Jeff Whitaker, and Gary Bates

ESRL Physical Sciences Division

What is a reforecast?

A "hindcast," a large set of weather or climate predictions *using the same model and data assimilation system that is used to make the real-time forecasts*.

Why generate reforecasts?

Weather and climate models often have large systematic errors. To provide useful decision support to customers, forecasts must be as accurate and reliable as possible. Reforecasts facilitate the "calibration" of weather forecasts, the post-processing to statistically adjust today's forecast using the discrepancies between past forecasts and observations.

What makes this different from MOS?

"MOS" is Model Output Statistics, a similar technique used by NOAA's Meteorological Development Lab for producing statistically corrected forecasts based on NCEP's models. Whereas MOS uses whatever training data is available from NCEP, sometimes a very short training data set given the ever-changing NCEP models, our purpose was to explore what can be done when a *very large training data set* from a frozen model is available. Also, we have developed more sophisticated statistical techniques for post-processing than were used in MOS. The large training sample size from reforecasts is shown to be especially helpful in statistically adjusting forecasts for rare events (e.g. heavy precipitation) and forecasts at long leads.

What reforecast data sets have been computed?

First, a reforecast from a T62L28 (~250 km grid spacing) version of the NCEP GFS from 1998. 15-member ensemble forecasts have been computed out to 15 days lead for every day from 1979 to present. Since generating this data set, NCEP/EMC's Climate Forecast System Reanalysis and Reforecast (CFSRR) has been produced, configured using lessons learned from our 1st-generation reforecast ECMWF produces reforecasts in real time following our work. And we expect to do a next-generation reforecast for NCEP's current operational Global Ensemble System.

Weather-climate applications

Improving forecasts at long leads is a difficult problem of determining what forecast signal is there hidden in the noise created by the chaotic growth of initial condition errors and model error. We successfully demonstrated that reforecast-based products were more skillful than the operational 6-10 day and week-2 forecast produced by the NCEP Climate Prediction Center (CPC). As a result, CPC now uses our reforecast products.

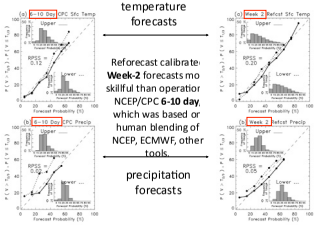

Example: La Conchita, CA mudslide, 1/12/05

notice very high probabilities of above-normal precipitation forecast over California

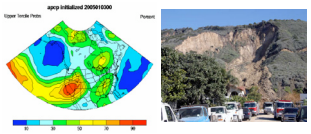

Selected references

Hamill, T. M., J. S. Whitaker, and X. Wei, 2004: Ensemble re-forecasting: improving medium-range forecast skill using retrospective forecasts. *Mon. Wea. Rev.*, **132**, 1434-1447.

Hamill, T. M., J. S. Whitaker, and S. L. Mullen, 2006:Reforecasts, an important dataset for improving weather predictions. *Bull. Amer. Meteor. Soc.*, **87**,33-46.

Hamill, T. M., and J. S. Whitaker, 2006: Probabilistic quantitative precipitation forecasts based on reforecast analogs: theory and application *Mon. Wea. Rev.*,**134**, 3209-3229.

Wilks, D. S., and T. M. Hamill, 2007: Comparison of ensemble-MOS methods using GFS reforecasts. *Mon. Wea. Rev.*, **135**, 2379-2390.

Hagedorn, R, T. M. Hamill, and J. S. Whitaker, 2008: Probabilistic forecast calibration using ECMWF and GFS ensemble forecasts. Part I: 2-meter temperature. *Mon. Wea. Rev.*, **136**, 2608-2619.

Hamill, T. M., R. Hagedorn, and J. S. Whitaker, 2008: Probabilistic forecast calibration using ECMWF and GFS ensemble forecasts. Part II: precipitation. *Mon. Wea. Rev.*, **136**, 2620-2632.

Hagedorn, R., R. Buizza, T. M. Hamill, M. Leutbecher, and T. N. Palmer, 2010: Comparing TIGGE multi-model forecasts with reforecast-calibrated ECMWF ensemble forecasts. Mon. Wea. Rev., in review.

Heavy-precipitation applications

Producing accurate, reliable forecasts of heavy precipitation can be difficult for many reasons. Raw forecast model output is commonly biased, and the forecasts may not be able to be computed at high-enough resolution to predict the small-scale features. With a large training sample size available from reforecasts, it is possible to make statistical adjustments to heavy precipitation forecasts, statistically downscaling the forecasts and dramatically improving forecast skill. Because of the success with reforecasts, the NCEP Hydrometeorological Prediction Center uses reforecast-based products to improve their quantitative precipitation forecasts.

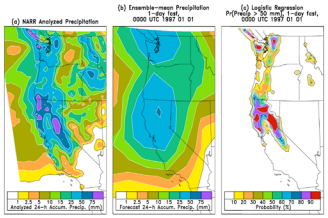

Example of the statistical downscaling and calibration that is possible using reforecasts. Left panel shows the analyzed precipitation; middle panel shows the ensemble-mean precipitation forecast, and right panel the calibrated probability of greater than 50 mm precipitation using the ensemble-mean data as a predictor.

What comes next?

We will generate a new reforecast data set with a current-generation version NCEP global ensemble system. We will: (a) make it available for post-processing research at ESRL, EMC, MDL, and universities. Here at ESRL, we will to use the data set to develop prototype applications for long-lead severe weather threats, aviation-related products, and renewable energy applications (solar output, wind-energy potential) (b) use it to define how NCEP should compute reforecasts operationally in future years. With a reforecast available every day, for example, we can determine how much worse the statistical post-processing performs for crucial applications with a sample every second day, or every third day. (c) Collaborate with hydrological colleagues, e.g. NOAA's Office of Hydrologic Development, to develop calibrated probabilistic ensemble streamflow guidance using the reforecasts. (d) Test whether the data set is useful for removing bias in data assimilation.

Will reforecasts provide as much benefit with newer models?

To explore this, we worked with colleagues at ECMWF to test the benefit of reforecasting with their ensemble prediction system. We found that (1) there was still a very large benefit to applying the reforecast technology to their system; and (2) our old, 1998 model with calibration provided through reforecasts provided more skillful probabilistic guidance than their ensemble prediction system without calibration. (3) The impact of the large training sample size was greater for rare events (heavy precipitation) than it was for more common events (light precipitation).

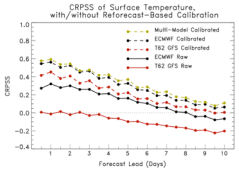

illustration of the skill of surface temperature forecasts from ECMWF and GFS reforecast systems, before and after reforecast calibration.

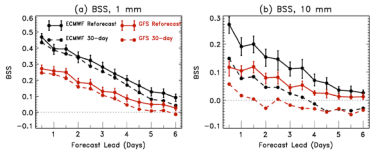

Precipitation Brier skill scores for (a) light precipitation (1 mm/day) and (b) heavier precipitation (10 mm/day), before and after reforecast calibration. Notice the greater impact of the reforecast calibration for the 10-mm event.

Multi-model ensembles instead?

ECMWF, with reforecast calibration, produced as good or better temperature forecasts than were obtained through a multi-model combination and calibration using a shorter, 30-day training data set.

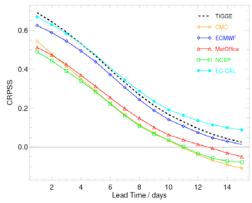

Calibrated ECMWF reforecast temperature skill (light blue) was generally as good or better than individual models' skill and the 30-day calibrated multi-model combination.

Prospects for Improving Subseasonal Predictions

Kathy Pegion and Prashant D. Sardeshmukh
Climate Diagnostics Center/CIRES/CU and Physical Sciences Division/ESRL/NOAA

Introduction and Motivation

1. **How skillful are state-of-the-art coupled GCMs at making Week-2 and Week-3 forecasts in the Tropics and Extratropics?**

   We compare the forecast skill of two CGCMs (NASA and NCEP) with the skill of simple **Linear Inverse Models** (LIMs), based on observed lag-covariances in the Tropics (of OLR) and Extratropics (of Ψ_{200} and Ψ_{850}).
2. **What is a realistic predictability estimate for this timescale?**

   We estimate the expected anomaly correlation forecast skill using the CGCMs and LIMs under a "perfect model" assumption, and argue that the LIM-based predictability estimates are more accurate.
3. **Are forecasts reaching a predictability limit for these timescales?**

   We compare the GCMs' actual forecast skill with our predictability estimates.

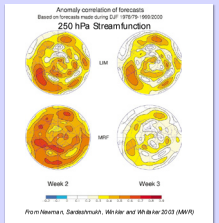

From Newman, Sardeshmukh, Winkler and Whitaker 2003 (MWR)

The NCEP Medium range Forecast (MRF) model was unable to outperform a LIM for forecasts of 250hPa streamfunction at Week 3.

Do the new (and coupled) GCMs perform better ?

Models and Data

CGCM Hindcasts used

Model	AGCM	OGCM	Hindcasts	Initialization
NASA/ GEOS5	GEOS5 2x2.5x72	MOM4 360x200x50	6-month hindcasts from 1980-2005	Daily 21z from replay runs
NCEP/ CFS03	GFS T62L64	MOM3 1x1/3x40 (10S-10N); increasing to 1x1x40 poleward of 30°	9-month hindcasts from 1981-2005	15 times per month from R2 (atm) and GODAS (ocn)

Reanalyses & OLR Datasets used

Data Set	Years Used	Resolution (lon x lat)
NCEP/NCAR Reanalysis (R1)	1980-2008	2.5x2.5
NCEP/DOE Reanalysis (R2)	1980-2008	2.5x2.5
ERA40 Reanalysis	1980-2001	2.5x2.5
20th Century Reanalysis	1980-2005	2.5x2.5
MERRA Reanalysis	1980-2005	2/3x1/2
JRA25 Reanalysis	1980-2008	2.5x2.5
NOAA/AVHRR OLR	1980-2008	2.5x2.5

Linear Inverse Model (LIM)

General Description

Assume the system can be described as:

$$\frac{dx}{dt} = Bx + \text{ stochastic noise}$$

The solution is:

$$x(t+\tau) = \exp(B\tau)x(t) + \varepsilon$$

The best forecast (in a least squares sense) is:

$$x(t+\tau) = \exp(B\tau)x(t)$$

For more details see Penland and Sardeshmukh 1995 (J. Clim)

Implementation of LIM

Define a reduced system anomaly state vector

$$X = \begin{bmatrix} \Psi \\ H \end{bmatrix}$$

Ψ = 200mb and 850mb NH streamfunction anomalies for DJF (30 EOFs)
H = Tropical OLR anomalies for DJF (7 EOFs)

In practice, X also needs to be coarse-grained & time averaged

1. Interpolate to a 7.5 x 3.5 deg grid.
2. Use 7-day running means.

Make Forecasts : $x(t+\tau) = \exp(B\tau)x(t)$

1. Estimate B (from observed and Reanalysis data) $B = \frac{1}{\tau}\left[C(\tau)\,C^{-1}(0)\right]$
2. Cross-Validate forecast skill through "jackniffing"

See Winkler, Newman, and Sardeshmukh 2001 (J. Clim) and Newman, Sardeshmukh, Winkler, and Whitaker 2003 (MWR)

LIM Local Anomaly Correlation Skill

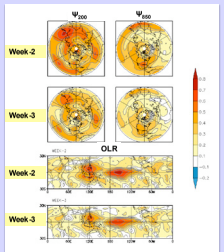

The LIM is a skillful model that provides a good baseline for assessing the skill of the CGCMs

Dynamical Model Skill

Difference in Anomaly Correlation Skill : CGCM skill *minus* LIM skill

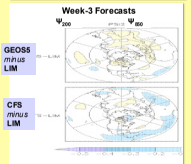

LIM remains a challenging benchmark for CGCMs to beat at Week-3 in the extratropics

Difference in Anomaly Correlation Skill : GEOS5 7-member Lagged Average Ensemble *minus* LIM

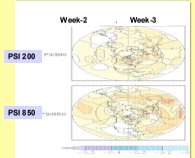

A "poor man's" 7-member lagged-average ensemble forecast is made from the GEOS5 forecasts. The skill of the ensemble-mean forecast is generally higher than the LIM skill in the extratropics at both Week 2 and Week 3 .

Taylor Diagram Summary of CGCM and LIM Skill

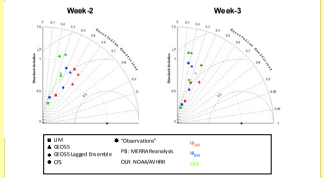

For all variables and models, anomaly correlation skill at these forecast ranges is generally very low (mostly < 0.5). This low skill limits the utility of the forecasts. What are the prospects for skill improvement? To address this, it would be nice to have estimates of the *potential* skill.

Predictability

Predictability is the expected skill of infinite-member ensemble-mean forecasts using a "perfect model"

Signal-to-noise ratio:

$$S = \frac{\|\text{ensemble mean anomaly}\|}{\|\text{ensemble spread}\|}$$

Expected Anomaly correlation skill of a Perfect Model, n-member ensemble:

$$\rho_n(\tau) = \frac{S^2(\tau)}{\left\{\left[S^2(\tau)+1\right]\left[S^2(\tau)+\frac{1}{n}\right]\right\}^{1/2}}$$

See Sardeshmukh, Compo and Penland. 2000 (J. Clim) & Compo and Sardeshmukh 2004 (J. Clim) for details

For GEOS5:

S is calculated directly from the 7-member lagged ensembles

For LIM:

The variance is partitioned into the part due to the signal and the part due to the noise

$$F = diag\left[G(\tau)C(0)G^T(\tau)\right] \quad \text{= Signal Variance}$$

$$E = diag\left[C(0) - G(\tau)C(0)G^T(\tau)\right] \quad \text{= Noise Variance}$$

$$S^2 = \frac{F}{E}$$

Predictability Estimates

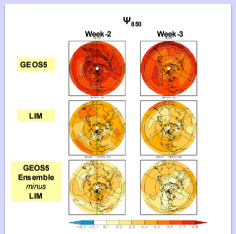

GEOS5 ensemble-based predictability estimates are ~ 0.3-0.4 higher than the estimates made from the LIM. Is this realistic?

Understanding Difference in Predictability

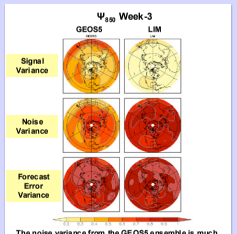

The noise variance from the GEOS5 ensemble is much smaller than the forecast error variance, indicating that it is underestimated. However, the LIM noise variance is similar to its forecast error variance.

Understanding Difference in Predictability

Difference Between Model and Reanalysis Autocorrelations Ψ_{850}

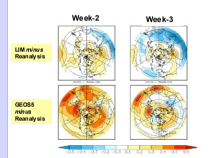

The GEOS5 autocorrelations are generally higher than in the Reanalysis, indicating that the model is more persistent than observed, leading to an overestimated signal.

How much Predictability is left to be realized?

Difference Between GEOS5 Lagged Ensemble Skill and LIM-based Predictability Estimates

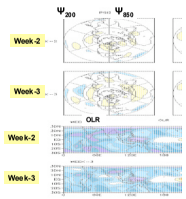

In the extratropics, there is little skill left to be realized.

Conclusions

1. An ensemble forecasting system is needed for the CGCMs to outperform the LIM at Week-3.
2. Traditional "perfect" model predictability estimates using a CGCM overestimate the magnitude of the forecast signal and underestimate the magnitude of the noise leading to inflated predictability estimates.
3. The LIM provides a more realistic "lower upper bound" for potential skill than the lagged average ensemble from GEOS5.
4. For NH streamfunction and central Pacific OLR, there is apparently little skill left to be realized *on average*.

Forecasts on these timescales should be focused on making "forecasts of opportunity", i.e. when the forecast signal is identified *a priori* to be relatively large

Distinct Causes for Two Principal U.S. Droughts of the 20th Century

Martin Hoerling[1], Xiao-Wei Quan[1,2], and Jon Eischeid[1,2]
[1]NOAA/ESRL/PSD, [2]CIRES/University of Colorado at Boulder

Observations

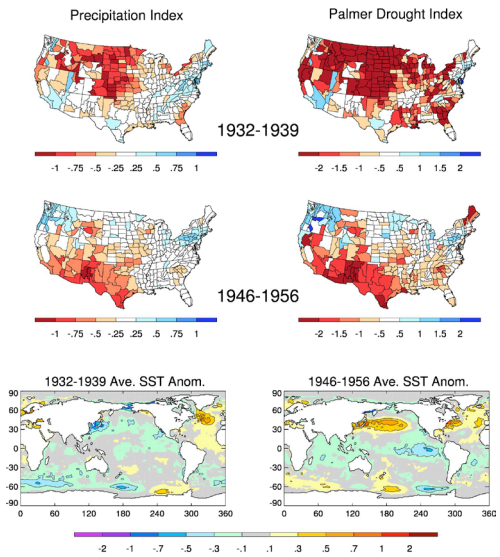

Q1: Did the different SST conditions prevalent during the 1930's vs. the 1950's cause the different spatial expressions of drought?

Q2: What are key features of a U.S. drought early warning system?

Simulations

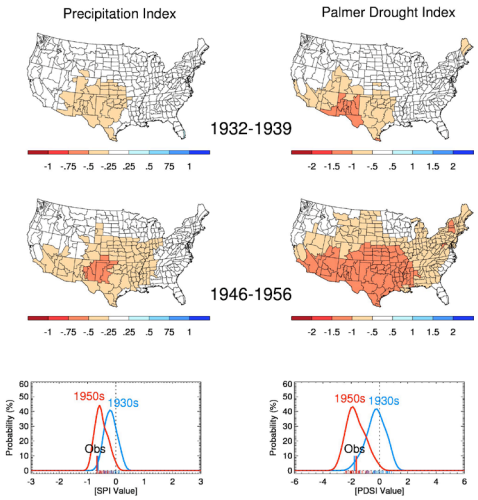

A1: Climate models indicate that drought severity over the Northern Plains during the 1930's was likely triggered by random atmospheric variability. The 1950's Southern Plains drought was strongly ocean forced.

A2: The Southern Great Plains lie in an epicenter of potentially skillful drought prediction for which an ocean observing system would constitute early warning.

Regional Experimental Seasonal Forecast Guidance: A 10-year Track Record in the Southwestern U.S.

Klaus Wolter
NOAA-ESRL, Physical Science Division, and CIRES, University of Colorado at Boulder
klaus.wolter@noaa.gov

Motivation

1. Climate Prediction Center (CPC) forecast skill over the Interior West 'leaves room for improvement' for seasonal precipitation forecasts.

2. Recent severe drought conditions have made such forecasts more relevant - water managers are more motivated to utilize climate forecast information.

3. Is there anything reliably usable beyond ENSO for this region?

Can we get some of this 'climate puzzle' figured out before 'Global Change' alters everything?

The Trouble with Climate Divisions

Traditional Climate Divisions cover the U.S. unevenly, as one goes from east to west, and even from one state to another (Colorado vs. Wyoming!). Several statistical climate prediction schemes at CPC were originally based on climate divisions in the West.

January-March correlations between Climate Divisions and COOP (left)/ SNOTEL (right) precipitation values are lowest in the interior of the U.S., in particular along the spine of the Rockies (during one of the best seasons).
If we want to get away from looking at the predictive climate signal 'through coke-bottles', more coherent climate divisions can only help!

Can We Improve Upon Status Quo?

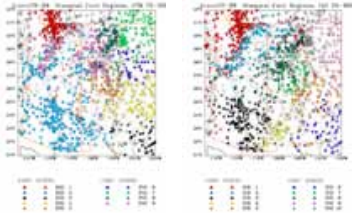

Improved seasonal **PREDICTANDS** based on COOP and SNOTEL station data were first developed in 2000-01, using multivariate techniques such as Cluster Analysis and Rotated Principal Components. The amount of color in each station symbol is proportional to locally explained variance via core index time series. Better predictands (higher signal-to-noise ratio) accomplish at least better down-scaled representation of ENSO associations.

Customized **PREDICTORS**: Regional SST in eastern Pacific and western Atlantic Ocean basins, preceding moisture history, and non-ENSO teleconnections (Indian Ocean!) - all had to have been established in previous analyses, or be 'intuitive'. Predictors were **not** optimized to **avoid overfitting**.

The prediction technique employed here is fairly old-fashioned: **stepwise linear regression** (SLR), with a 10% increase in explained variance requirement, and decadal cross-validation (poor man's ensembles; 6 sets of prediction equations).

Frequently Used (and Skillful) Predictor Regions

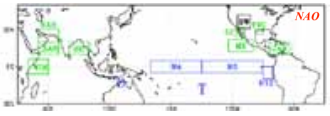

Robust PREDICTORS that show up repeatedly in these experimental seasonal precipitation forecast schemes (cross-validated WY'51-99 or verified WY'00-09 Heidke Skill Scores ≥30). Aside from '**flavors of ENSO**' (in blue), the **Indian Ocean** stands out with four important SST regions that show strong teleconnections with our predictands. **Nearby SST** may achieve skill by influencing regional moisture transports. The **NAO** plays a frequent role as well, possibly via altering North Atlantic SST.

A priori cross-validated skill

Bias-corrected ensemble (5 separate decades held out) Heidke skill scores (HSS) within the 1951-99 training period. Hindcasts are based on climate division predictands developed separately for four cardinal seasons (JFM - OND). Forecast equations frozen in 2003.

Season	<HSS>	Number of HSS ≥0.15/≥0.30	Highest HSS
JFM (9)	24	4 / 4	0.53 in NC CO
AMJ (9)	13	2 / 1	0.31 SE AZ-S NM
JAS(10)	16	5 / 0	0.28 in NE CO
OND (6)	17	4 / 0	0.28 in NM
All (34)	18	15 / 5	<Best / Worst>

One Decade of Seasonal Forecast Guidance

WY 2000-2009 verification skill

Heidke Skill Scores (HSS) calculated for ALL ensemble forecasts, and forecasts with ≥3% shifts at 0.5 month leads. Near-neutral forecasts had to have both extreme tercile probabilities suppressed to be counted.

Season	HSS ALL/3%	#0.15 (0.30)	Coverage (at 3%)
JFM (9)	5/ 7	3 (2)	93%
AMJ (9)	7/ 9	5 (3)	73%
JAS (10)	16/22	5 (5)	78%
OND (6)	5/ 9	3 (1)	70%
All (34)	8/12	16(11)	79%

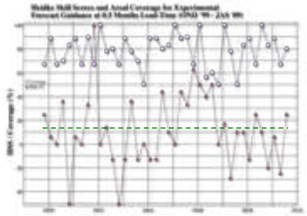

Tercile verification HSS for tilts of at least 3% (red) as well as their areal coverage (purple) ensemble forecasts at 0.5 month lead-time for Water Years 2000-2009. Green stippled line indicates average skill score in last decade.

Full training period forecasts were inferior to **ensemble** forecasts in all seasons but Fall (OND).

Fall season has been the hardest season to predict, both in hindcast testing, as well as over last decade.

Increasing the probability shift requirement from 3% to 7% increases forecast skill only marginally, but drops almost half of the **areal coverage**, which is one of the main improvements over CPC forecast skill.

First year of public forecasting (**2002**) was literally a 'trial by fire' in Colorado, since forecast skills were so low in that record-wildfire year. Nevertheless, stakeholders understood that this was an experimental product, and were pleased that its low skill was transient.

Seasonal Highlights

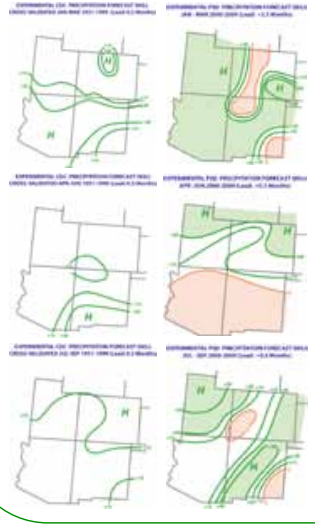

Tercile cross-validated (left) and verification (right) skill in ensemble forecasts for **January-March**. This is the season with the clearest preference for a longer lead (**3.5 months**), with an average HSS=20. *Poor verification skill in NC Colorado!*

April-June: Highest *a priori* forecast skill region in southern NM has verified poorly since 2000, while a strip from northern UT into the NE panhandle stands out with HSS ≥ 30. This season is seasonably dry in AZ/NM compared to further north.

July-September: Most positive surprise: verification skill in UT and from southwestern NM to eastern CO has been much better than expected, while AZ, southeast NM, and southwest CO remain poorly predictable.

Conclusions

1. **Seasonal forecast skill for the interior southwestern U.S. appears to be linked not only to ENSO, but also to select other SST regions (Upstream + Indian Ocean). In fact, predictive skill in the ENSO context appears associated with 'flavors of ENSO' rather than mainstream ENSO indices such as Niño 3.4 ('ONI') SST.**

2. **Cross-validated hindcast skill is largest in winter, and lowest in spring, consistent with CPC's experience. However, fully independent verification for the last decade has revealed some surprises: low skill at 0.5 month lead-time for the winter, but much better at 3.5 months; best overall skill during the monsoon season. All seasons feature at least some regions with high verified skill (HSS≥30).**

3. **Except for fall, bias-corrected ensemble forecasts outperformed full training period regression forecasts. Filtering out forecast tilts under 7% increases overall skill only marginally, while dropping more than 40% of the coverage achieved with a 3% tilt requirement. Many, but not all 0.5 lead-time forecasts outperform forecasts issued earlier.**

4. **National new climate divisions have been developed, and could be tested in a much wider geographical range of prediction experiments, such as California and the Western U.S. in general. Meanwhile, current forecast guidance can be found at:** ***http://www.esrl.noaa.gov/people/klaus.wolter/SWcasts/***

   and new national climate divisions at: ***http://www. esrl.noaa.gov/people/klaus.wolter/ClimateDivisions/***

International Comprehensive Ocean-Atmospheric Data Set (ICOADS)

Scott Woodruff[a], Sandra Lubker[a], Steve Worley[b] and Eric Freeman[c]

a) NOAA/ESRL/PSD b) NCAR c) NOAA/NCDC

Evolving Spatial Coverage

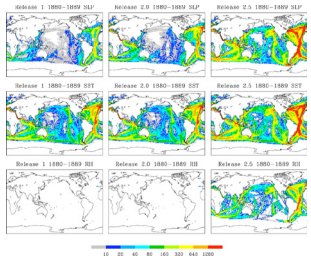

Decadal (1880–1889) totals of sea level pressure (SLP) observations (upper) illustrating data additions between Releases 1 (completed in 1985), 2.0 (2002), and 2.5 (2009) (R2.5). The colors show the number of observations in a 2° box per decade. Grey indicates 1–10; dark blue indicates 11–20; …; orange indicates 641–1280; red indicates 1281 or more. (Middle and Lower) As for (upper) except for sea surface temperature (SST) and relative humidity (RH).

Evolving Temporal Coverage

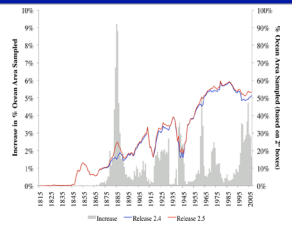

(Right axis) Annual percentage ocean area sampled for SST for R2.5 (red curve) compared to the previous Release (R2.4) (blue curve). (Left axis) Annual percentage increase in global ocean area sampled for R2.5, compared to R2.4 (bars).

Evolving Platform Mixture

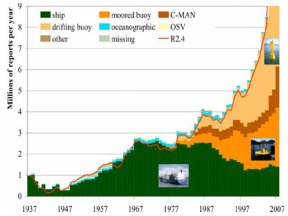

Annual distribution (1937–2007) of major platform types in R2.5 shown as millions of reports per year. For clarity the vertical scale is truncated at 9M; years 2005–07 have 13M, 15M, and 16M total reports (not visible) in R2.5, respectively. The red line curve contrasts the R2.4 annual counts. Ships (mainly VOS plus some R/Vs), buoys and oceanographic are self explanatory. Ocean (permanent) Station Vessel = OSV, Coastal–Marine-Automated Network = C-MAN; ocean drilling rigs/platforms and other small entities = other; and unidentified platform types = missing. (Figure adapted from Woodruff et al. (2008); ship photo courtesy of www.ShipPhotos.co.uk).

Project Background

As the result of a US project starting in 1981, available global surface marine data from the late 17th century to date have been assembled, quality controlled, and made widely available to the international research community in products of the Comprehensive Ocean-Atmosphere Data Set (COADS). A new name, International COADS (ICOADS), was agreed in 2002 to recognize the multinational input to the blended observational database and other benefits gained from extensive international collaboration, while maintaining continuity of identity with COADS, which has been widely used and referenced.

ICOADS has grown from a US-centric effort between NOAA—its ESRL Physical Science Division (PSD) and National Climatic Data Center (NCDC)—and the National Center for Atmospheric Research (NCAR), to an expanded US and international partnership. The NOAA portion of ICOADS is partially funded by the NOAA Climate Program Office (CPO).

Blended/Candidate Data Source

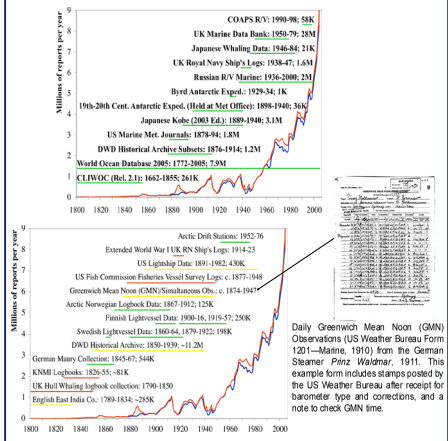

Daily Greenwich Mean Noon (GMN) Observations (US Weather Bureau Form 1201—Marine, 1910) from the German Steamer *Prinz Waldmar*, 1911. This example form includes stamps posted by the US Weather Bureau after receipt for barometer type and corrections, and a note to check GMN time.

(Top) Major historical data sources added to R2.5 (Woodruff et al. 2010a). Horizontal green lines illustrate the time range of the original data sources. The annual numbers of reports are plotted as curves, blue for the previous R2.4, and red for R2.5. For clarity the vertical scale is truncated at 9M; years 2005-07 have 13M, 15M, and 16M total reports (not visible) in R2.5, respectively. Data coverage prior to 1800 is very sparse. (Bottom) Similar to (Top), the time periods of candidate historical data to be blended into ICOADS are spanned by horizontal colored lines: green candidates are fully digitized but require format translation, yellow are partially digitized, and red are in the planning stages for digitization. Each dataset name is appended with the date range and approximate number of reports (if known) (from Wilkinson et al. 2010).

Evolving National Data Mixture

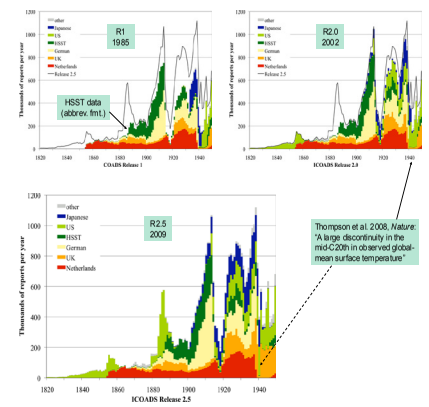

Thousands of reports per year for 1820-1949 available in Releases 1 (issued in 1985), 2.0 (2002), and 2.5 (2009), stratified by national sources, and from the Historical SST Data Project (HSST). The annual numbers of reports in R2.5 are also plotted as a curve for R1 and R2.0 to highlight the later gains. Thompson et al. (2008) identified a large discontinuity c. 1945 arising from abrupt national data mixture changes based on R2.0 data.

Recent ICOADS and Related Publications

- Brohan, P., R. Allan, J.E. Freeman, A.M. Waple, D. Wheeler, C. Wilkinson, and S. Woodruff, 2009: Marine observations of old weather. *Bull. Amer. Meteor. Soc.*, **90**, 219-230.
- Charpentier, E., D.E. Harrison, J.R. Keeley, E. Kent, M. Mietus, N. Rayner, M. Rutherford, V. Swail, and S, Woodruff, 2008: Third JCOMM Workshop on Advances in Marine Climatology (CLIMAR-III). *MeteoWorld*, December 2008.
- Kent, E., S. Woodruff, N. Rayner, T. Arbetter, C. Folland, F. Koek, D. Parker, R. Reynolds, R. Saunders, V. Smolyanitsky, S. Worley, and T. Yoshida, 2007: Advances in the use of historical marine climate data (Second International Workshop on Advances in the Use of Historical Marine Climate Data). *Bull. Amer. Meteor. Soc.*, **88**, 559-564.
- Thompson, D. W. J., J. J. Kennedy, J. M. Wallace, and P. D. Jones. A large discontinuity in the mid-twentieth century in observed global-mean surface temperature. *Nature*, **453**, 646-649 (2008).
- Wilkinson, C., S.D. Woodruff, P. Brohan, S. Claesson, E. Freeman, F. Koek, S.J. Lubker, C. Marzin, and D. Wheeler, 2010: RECovery of Logbooks And International Marine Data: The RECLAIM Project. *Int. J. Climatol*. (in press).
- Woodruff, S.D., H.F. Diaz, E.C. Kent, R.W. Reynolds, and S.J. Worley, 2008: The evolving SST record from ICOADS. In *Climate Variability and Extremes during the Past 100 Years* (S. Broennimann, J. Luterbacher, T. Ewen, H.F. Diaz, R.S. Stolarski, and U. Neu, Eds.), Advances in Global Change Research, Vol. 33, Springer, 65-83.
- Woodruff, S.D., S.J. Worley, S.J. Lubker, Z. Ji, J.E. Freeman, D.I. Berry, P. Brohan, E.C. Kent, R.W. Reynolds, S.R. Smith, and C. Wilkinson, 2010a: ICOADS Release 2.5: Extensions and Enhancements to the Surface Marine Meteorological Archive. *Int. J. Climatol*. (in press).
- Woodruff, S.D., N. Scott, D.I. Berry, M.A. Bourassa, E. Charpentier, S. Gulev, H. Haar, E.C. Kent, R.W. Reynolds, G. Rosenhagen, M. Rutherford, V. Swail, S.J. Worley, H.-M. Zhang, R. Zöllner, 2010b: Surface In situ Datasets for Marine Climatological Applications. In *Proceedings of OceanObs'09: Sustained Ocean Observations and Information for Society (Vol. 2)*, Venice, Italy, 21-25 September 2009, Hall, J., Harrison D.E. & Stammer, D., Eds., ESA Publication WPP-306 (in press).
- Worley S.J., S.D. Woodruff, S.J. Lubker, Z. Ji, J.E. Freeman, E.C. Kent, P. Brohan, D.I. Berry, S.R. Smith, C. Wilkinson, and R.W. Reynolds, 2010: The Role of ICOADS in the Sustained Ocean Observing System. In *Proceedings of OceanObs'09: Sustained Ocean Observations and Information for Society (Vol. 2)*, Venice, Italy, 21-25 September 2009, Hall, J., Harrison D.E. & Stammer, D., Eds., ESA Publication WPP-306 (in press).